D2AM, status and highlights of the French anomalous CRG beamline at ESRF.

presented by J.-François Bérar

May 11, 2004

This document is the collective work of all those participating in the beamline. They are to be thanked for their written contributions and for their help and comments in preparing this booklet.

Contents.

Introduction **2**

1 Beamline presentation **2**
- 1.1 Staff and associated laboratories 2
- 1.2 User access to the D2AM beamline. 3
- 1.3 Optics and instrument overview 3
- 1.4 Future perspectives and plans for upgrading 4

2 Scientific results **6**
- 2.1 DAFS, a probe of local environment in complex samples . 6
- 2.2 Applications of anomalous scattering at wide angles . . . 8
- 2.3 Diffuse scattering and weak signals 10
- 2.4 High resolution and Coherent scattering at BM2 11
- 2.5 Soft condensed matter 12
- 2.6 In situ materials science and engineering 16
- 2.7 Detector development 18

Appendices **21**
- Grazing-incidence DAFS of self assembled quantum wires. . . 21
- Melting behavior of levitated Y_2O_3. 21
- Structural evidence for the Ta tetamerisation displacement..... 22
- Phason elastic constants ... from diffuse scattering measurements 22
- Statics and kinetics of ... transition in the $AuAgZn_2$ alloy. 23
- SAXS ... of silica and carbon replicas with ordered porosity. . . 23
- Morphological investigation of ... Activated Carbons. 24
- References 2004-2001 24

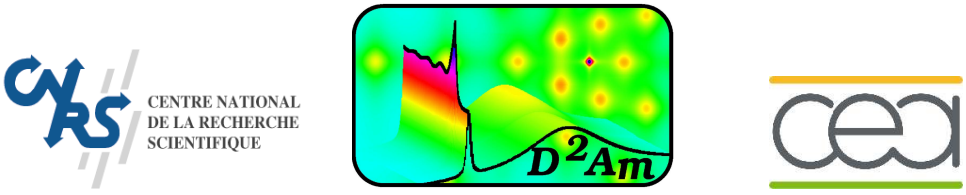

Introduction

Built to respond to a broad range of problems in materials science, the D2AM (**D**iffraction et **D**iffusion **A**nomale **M**ultilongueurs d'onde) beamline quickly focussed an important part of its activity on selected methods involving either anomalous scattering, high resolution or coherence. It remains however completely open to all materials science subjects, as can be seen from the contents of the section on scientific results, such as diffuse scattering, soft condensed matter, material engineering, ...

Its design as an anomalous beamline allows the wavelength to be changed easily and has encouraged some researchers to exploit not only the anomalous contrast but also the whole of the absorption fine structure in diffraction using DAFS. After the first experiments on orbital ordering in bulk materials they progressed to 2 dimensional structures such as multilayers, epilayers and then to quantum wires or quantum dots. Encapsulated dots in semiconductors are now being investigated.

At the same time, scientists engaged in SAXS experiments have taken advantage of the coherence of our bending magnet beam and defined the experimental protocol needed to obtain the requisite quality of the beam. This work is the basis of our high resolution SAXS configuration, which extends the range of the instrument to cover that normally investigated by visible light scattering. By this means, anisotropically scattering systems can be investigated by virtue of the 2 dimensional detection.

After a brief outline of the beamline, this report to the 2004 ESRF review panel goes on to describe a selection of experiments that are representative of the variety of results obtained on D2AM in recent years. This is followed by a small number of complete papers. The entire list of publications for the years 2001-2004 is given in an Appendix; other significant papers are referenced in the text.

1 Beamline presentation

A French CRG beamline

The CRG beamlines at the ESRF were founded by the CEA and CNRS in France in order to facilitate access of the French community to synchrotron radiation. The D2AM beamline was dedicated to anomalous scattering and studies of diffuse scattering at small or high angles. This project received strong support from laboratories in the Grenoble area.

The beamline was built to reconcile three experimental instruments, each sharing the beam time : a diffractometer dedicated to protein crystallography, a small angle camera and a materials science goniometer. The optics were designed to satisfy the common requirements of these groups : the project leaders, *J.P. Simon (CNRS)* and *M. Roth (CEA)* attached particular concern to the signal-to-noise ratio.

The beamline was among the first ESRF beamlines to open to users, in September 1994. Its scientific activity was reviewed in May 1997. As a result of the increased demand for protein crystallography, a new French CRG beamline was constructed (FIP). After February 1998 D2AM was no longer the priority of the protein crystallography community and it can be now considered as a materials science station with two instruments :

- a small angle camera (responsible *J.P. Simon*),
- a 7-circle goniometer (responsible *J.F. Bérar*).

At the present time, about 1/3 of the beam time is dedicated to the small angle scattering camera while the remaining 2/3 involve the goniometer.

The annual budget allocated by the CNRS and the CEA in 2002 amounted to 218 kE and in 2003 to 190kE. This budget does not include staff salaries but takes into account all charges incurred to the ESRF, running costs and investisment, including our detector development program.

1.1 Staff and associated laboratories

As the D2AM beamline is a CRG, its organization differs slightly from that of ESRF beamlines, which enjoy the backing of the Experimental Division support groups. The beamline is managed by a small staff of 4 permanent CNRS employees (a scientist engineer having being appointed in 2001 to reinforce it).

S. Arnaud	*J.F. Bérar*	*N. Boudet*	*B. Caillot*
technician	responsible	scientist	engineer

In addition, the beamline receives support from Grenoble laboratories for development, support of external users and in-house research activities. About 10 scientists participate in these activities on a part-time basis, or about 2 - 3 full-time equivalent staff members. The support laboratories are:
- Laboratoire de Cristallographie (LDC)
- Laboratoire de Spectrométrie Physique (LSP)
- Laboratoire de Thermodynamique et Physico-chimie Métallurgiques (LTPCM)
- Service de Physique des Matériaux et Microstructures (SP2M).

The following figure shows for each of these four support laboratories those scientists who are most involved and their field of interaction with the beamline.

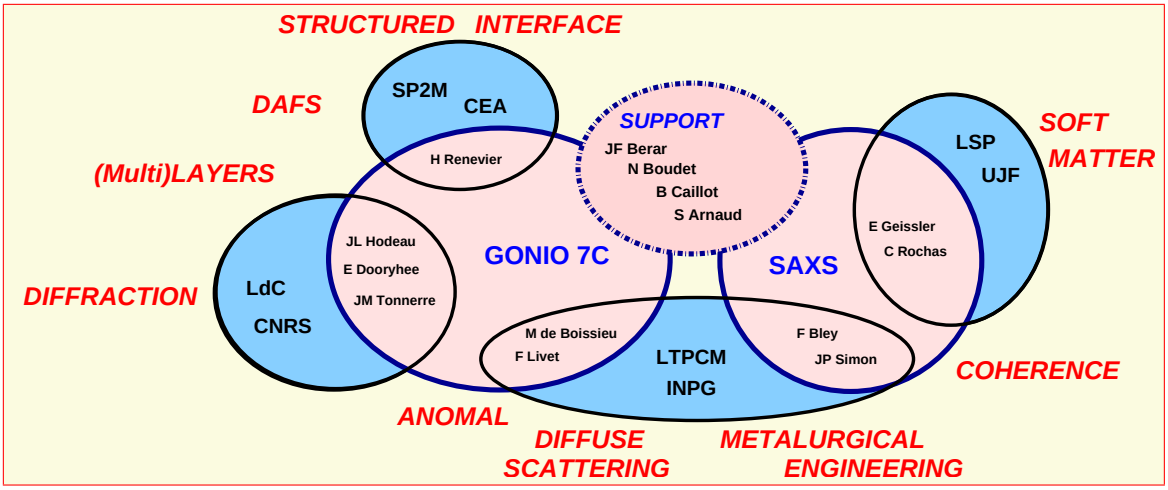

1.2 User access to the D2AM beamline.

From the point of view of users, access to the D2AM CRG beamline is similar to those of the ESRF. The "user dedicated time" is allocated by two different review committees : the ESRF committees allocate 1/3 of the time, while the French CRG committees allocate the remaining 2/3. The scientific topics correspond to those of the ESRF review committees : HS, ME, SC (CH, IN). The ratio between requested and allocated shifts (or proposals) is about 2-2.5.

	TOTAL		*ESRF*		*CRG*		
year	proposals	shifts	proposals	shifts	proposals	shifts	(requested)
2000	33	410	11	132+18	22	260	714
2001	42	474	10	132	32	342	759
2002	39	417	11	132	28	285	694
2003	36	428	11	131+15	25	279	617
2004(part)	23+x	413+x	4+x	63+(72)	19+x	238+(40)	535+x

Beamtime delivered to users by **review committees**

A few shifts reserved for teaching are distributed over about 5 days each year. Since 2001, one or two shifts each year are used by industrial companies under contract with the ESRF. Commissioning, maintenance and in-house research share the remaining time. In the period of reference, the allocated beamtime has been totally used by experiments. During these years very few experiments were interrupted by beamline failures (motors, cryostat) and this lost time has been replaced in the following months using beamtime reserved for maintenance.

1.3 Optics and instrument overview

For better stability with respect to energy, the D2AM optics is symmetrical, with a double monochromator situated between two mirrors. The beamline is located on the BM02 bending magnet and uses

the 0.85 Tesla source with a critical wavelength of 0.6 Å(20.6 keV). At the entry to the optical hutch, a primary collimator accepts up to $3mrad$ of the horizontal divergence. Primary slits located upstream of all the optical components are used to define the effective vertical and horizontal divergence. The first mirror, a platinium-coated silicon single crystal, acts as a low pass filter and enables the beam to be focussed in the vertical plane. These first elements lie in a very clean vacuum (10^{-9} without beam, $10^{-7}mbar$ with beam) that extends up to the last Beryllium window. The beam is then processed by a double crystal monochromator equipped with Si(111), or occasionally at high energies, with Si(311). This monochromator has a bandwidth of 10^{-4} and focusses the beam sagittally in the horizontal plane.

A second mirror, identical to the primary one, provides focussing in the vertical plane. Rear slits, located just after the second mirror and also near the instruments, reduce spurious signals from optical aberrations.

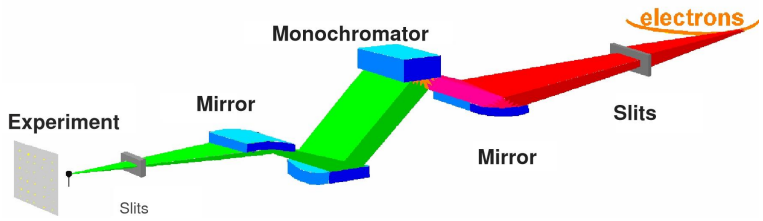

This whole symmetrical arrangement acts as fixed exit optics and should yield a 3:1 demagnification of the source. An exhaustive description has been published [1]. It delivers photons from 5 to 25 keV to the experimental hutch in a spot of a few hundred microns. Spots of $70 \times 100\ \mu m^2$ can be attained for experiments requiring a very small beam size.

The experimental hutch is equipped with a "7-circle" goniometer, which consists of an Euler cradle for the sample, a detector arm that can move in the plane vertical to the polarization and up to 75^o in the horizontal plane. All angles are driven by step motors with a resolution better than 0.001^o. A two circle analyser can be fixed on the detector arm. Attention has been paid to anciliary equipment : evacuated sample holder cell, displex, furnaces, etc., are available.

The small angle camera [2] is situated at the rear of the same experimental hutch and receives the incoming beam through an evacuated pipe passing inside the goniometer. The camera itself, on a single granite bench, consists of antiscattering slits, sample holders, exchangeable vacuum pipes up to the beam stop and a CCD detector. The sample-detector distance ranges from 0.3 m to $2m$, with a normal q range between $3.10^{-3}\mathring{A}^{-1}$ and $1\mathring{A}^{-1}$ between 8 and 15 keV and a flux of $5.10^{10} - 10^{11} ph/s$. Ultra small scattering has reached $4.10^{-4}\mathring{A}^{-1}$, thus providing complete overlap with standard visible light scattering. By contrast, experiments at high pressure or high temperatures need hard X-rays (up to $2\mathring{A}^{-1}$ at 20 keV). The flexibility of the camera has been put to advantage in several in-situ experiments in materials science and engineering as well as for Grazing Incidence SAXS.

Both instruments share detectors. These consist of scintillators/photomultipliers and cameras. The most commonly used is a CCD fiber optic coupled ($60 \times 50\ mm^2$). Since 1999, gas detectors have no longer been in use.

1.4 Future perspectives and plans for upgrading

To define realistic perpectives, it is essential to situate the place of the CRG beamlines in the context of the planned beamlines at ESRF and SOLEIL. Our major specific expertise lies in skillful use of a low noise, anomalous beamline in the range $5 - 25\ keV$. Instead of moving on to new and different physics, therefore, it seems to be both more pertinent and of more immediate urgency to improve the instruments so as to investigate more exacting samples, for instance, samples prepared by emerging technologies.

The optical parameters of the beammline were defined long ago, on the basis of the techniques available in 1994. Since its design, the ESRF source has increased in brightness. The beamline optics should keep abreast of these improvements in order to ensure the achievable beam quality for the experiment. A rejuvenation plan was submitted to our founding authorities for this purpose. The

[1] *J.L. Ferrer et al.* J. Synchrotron Rad. **5** (1998) pp 1346-1356
[2] *J.P. Simon et al.* J. Appl. Cryst. **30** (1997) pp 900-904

most sensitive element of our optics, the sagittal bender, was replaced in 1998, but we are now limited by the most onerous components of the beamline : the mirrors and the monochromators.

• **Mirrors -** Major improvments have been made in mirror technology since 1994. Our mirrors, made from a silicon single crystal coated by $50nm$ platinium, were polished to slope errors lower than 5 μrad(rms) and a roughness of 5 $\mathring{A}$(rms). Modern mirors attain 1 μrad and 1 $\mathring{A}$. The vertical structure of our beam appears complex, with a strong dependence on the resolution of the observation. It is probable that such structures are associated with intermediate frequencies coming from the slope errors. At present, to attain high resolution on D2AM the vertical aperture must be reduced to minimize this effect. Our mirrors need to be repolished and their bender optimized : this is the most important item in our rejuvenation plan. Simultaneous with this operation, the beryllium windows must be polished in order to remove the speckle pattern that they generate.

• **Monochromators -** The sagittal bender was replaced in 1998 by the "standard" ESRF design. This improved its reliability, eliminating the backlash associated with the friction between the pusher and the crystal holder. This gives us reproducible control of the curvature and permits dynamical foccussing in the energy scan, as is required in DAFS experiments. However due to its design, the focal point of a crystal with ribs is far from perfect. At high resolution two focal lengths are revealed : one associated with the ribs, the other with the intervening material. The consequence is to increase the horizontal size of the spot from 100 μm to 250 μm . This is a heavy penality for experiments that require very low noise, since one component cannot be removed from the focal plane. We therefore intend to improve the bending system of our monochromator to gain simultaneously in flux and purity.

As these considerations on the mirrors and the monochromator do not at present take into account the various "upgrade plans" that appear at the ESRF, some remarks are in order. We recall that the beamline is competitive in the range $5 - 25$ keV. This range, which allows edges of nearly all the elements to be reached, should be maintained. Another major virtue of the D2AM beamline is its long-term optical stability (greater than 24 h even in coherent operation). This property must also be preserved; it is one of the reasons for which we have not at present decided to move to cryogenic cooling of the monochromator.

• **The 7 circle goniometer** still has good precision on its motors since they are all coded. However it has been operating for 10 years : the 2θ movement is becoming hard and should be repaired. The sphere of confusion of the Euler cradle, repaired in 2002, is about $50\mu m$. However, since the Eulerian geometry of the sample cradle is not optimised for grazing incidence experiments, we decided to add a new circle this year to assist such experiments. Nevertheless, if this kind of experiment is to become more frequent in the long term, we must consider the choice of adding a dedicated goniometer in the experimental hutch. This must be done while keeping in mind that the most important contribution that D2AM can offer will come from measurements of weak or anomalous signals, as in DAFS.

• **The SAXS camera** is a very flexible instrument with various sample holders and in-vacuo vessels. There are, however, limits to its use, but we must focus our choice on the characteristics of this beamline camera and to ensure that the planned improvement will really be of help to the community. Although the signal-to-noise ratio is very good, a very weak background remains even without a sample; although it can be corrected for, it handicaps measurements of weakly scattering samples. Tests are in progress to identify the principal cause: the optics, the beam monitoring or the detector. The other limitations arise from beamstop size. 2D high resolution experiments stand to benefit from an increase of the sample-detector distance to 3 (4) meters.

These considerations on the instruments imply modifying and enlarging the experimental hutch, an operation that seems reasonable as the control room and user room are sufficiently wide and could be shortened.

• **Detectors -** The beamline started in 1994 with NaI:Tl scintillators associated with photo multipliers and gas detectors. An effort was made earlier to improve the detection efficiency with avalanche photo diodes but the effort was quickly directed towards 2D detection. Even though CCD detectors are far from ideal detectors for our application, a first scientific CCD (1242×1152) was bought in 1997. This camera became outdated and developed defects. It has since been replaced by a new one (1340×1300) in 2002. Owing to progress in CCD technology, its dark current has been strongly reduced, thus allowing longer exposures.

Nevertheless, the detectors currently available on the market are still far from making full use of the beam quality of modern synchrotron sources, mainly owing to their small dynamic range and relatively long read-out time. To overcome these defects we initiated the development of a hybrid pixel detector. This project is detailed in section 2.7.

2 Scientific results

To represent the variety of topics investigated at D2am over the last few years, some results presented below are the summary of an activity, while others are examples that illustrate selected points. These are the strong points of the beamline and come both from external users and from in-house research.

2.1 DAFS, a probe of local environment in complex samples

In the 90s, DAFS appeared as an opportunity for accessing local environements. Attemps were made to develop energy dispersive DAFS while one group, led by *H. Renevier (Grenoble)* favoured a monochromatic approach well suited to the optics of D2AM ***[H-5]*** .

Diffraction Anomalous Fine Structure (DAFS) spectroscopy uses resonant elastic x-ray scattering as an atomic-, shell- and site-selective probe that gives information on the electronic structure and the local atomic environment as well as on the long range ordered crystallographic structure. A DAFS experiment consists in measuring the elastic scattering intensity as a continuous function of the incoming x-ray beam energy in regions spanning absorption edges. Like X-ray Absorption Fine Structure (XAFS) spectroscopy, it provides information on the chemical state and the local environment of the resonant atom (also known as the anomalous atom), like X-ray Absorption Fine Structure (XAFS) spectroscopy. But in contrast to XAFS, it is a *chemical-selective* and *site-selective* spectroscopy. Like Multiple-wavelength Anomalous Diffraction (MAD), DAFS provides a means of recovering the phase of the structure factor, which is important for solving the long-range average crystallographic structure.

The requirements of the experiment are to measure the intensities as a function of the energy as fast as possible, with a monitor corrected signal-to-noise ratio as high as 1000 or more (comparable to a typical XAFS experiment), and without distortions of the spectra. Since the mechanical precision and stability of all motors is necessarily limited, we developed a feedback control of the sample rocking-angle position (based on a sample-holder that rocks the sample around the ω axis) for measuring the maximum intensity. To cope with and take advantage of the high counting rate on the monitor, the sample fluorescence, or the diffraction peak, we developed a detector based on photodiodes operating in photovoltaic mode at room temperature, which provides high linearity and very large dynamic range. To speed up the Energy-Scanned experiment we implemented a quick-DAFS (q-DAFS) procedure that allows counting during motor movements. The whole settings is described in ***[3-28]*** .

One of the most interesting DAFS studies [3] performed at the beamline was the attempt to investigate charge ordering in magnetite Fe_3O_4 by measuring the energy and azimuthal dependence (dependence upon the incoming x-ray beam polarization) of the *d*-glide plane (002) and (006) forbidden reflections, below and above the Verwey transition (125K), at the iron K-edge ***[E-9, T-14, 1-12, 1-13, 1-27]*** . We have observed a) virtual exitation-deexitation transition through dipolar-quadrupolar channels at the tetrahedral iron atom (A site), b) strong resonance at the $1s-4p$ energy transition due to the anisotropy of the dipolar scattering factor of the trigonal ($\bar{3}m$) octahedral iron atoms (B site) and c) for the first time, the extended part above the edge that has the same origin as the main resonance and exhibits oscillatory behaviour as a function of the energy. The analysis of the experimental data shows that the anomalous scattering factor is anisotropic but is identical for all the octahedral iron atoms at room temperature and remains unaltered across the Verwey transition. The conclusion was drawn that octahedral iron atoms in magnetite cannot be described as pure ionic Fe^{3+} or Fe^{2+} ions, either spatially or temporally.

Nanostructured semiconductors

For the last years DAFS spectroscopy has proven to be a very successful tool for studying the crystallographic structure of thin films, superlattices and interfaces ***[T-9, 3-15, 3-23, 1-17]*** . More recently DAFS in grazing incidence (GI-DAFS)

[3] Resonant "forbidden" reflections in magnetite by *J. Garcia et al.* Phys. Rev. Lett. 85, (2000), 578.

has been developed and used to study uncovered InAs quantum wires (QWrs) grown on InP(001) ***[1-16]*** [4] . The QWrs are aligned along the [1$\bar{1}$10] direction with a typical length above 5 μm, a height between 0.6 and 2 nm, a period of 20 nm with an equivalent InAs coverage of about 2.5 monolayers (fig.1). We measured the DAFS spectra at the maximum of the QWrs satellite reflections, near the (420) and (440) InP substrate Bragg peaks at the As K-edge (11867 eV). The measurements were performed in grazing incidence geometry, with an incidence angle kept constant slightly above the critical angle of InP (about 0.2°). Grazing incidence is mandatory to enhance the QWr scattering contribution with respect to the substrate contribution.

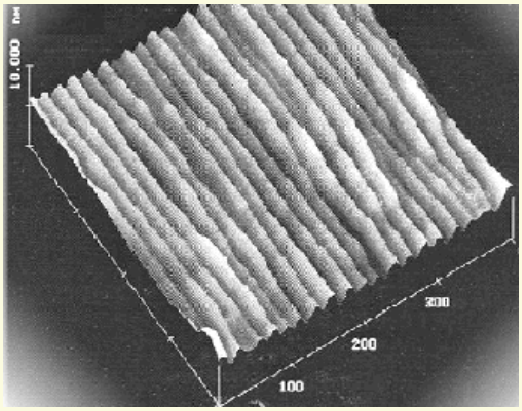

Figure 1: AFM tridimensional view of InAs quantum wires on InP buffer

We extracted the Extended DAFS oscillations that appear after the edge (fig.2a) and analysed them using an EXAFS data processing scheme to get local parameters such as distances and atomic populations. Theoretical multiple-scattering EXAFS signals were calculated by the FEFF code simulating the fine structure signal from an As atom inside a cluster containing In atoms, As_x and P_{1-x} atoms. The polarisation of the incoming photons was perpendicular to the surface, so that the contribution of the As and P next-nearest-neighbour atoms to EDAFS is due only to the out-of-plane atoms. Refinement of the data was completed by the least-square fit procedure of the FEFFIT program. The relevant results are the P concentration, $(1-x) = 0.4$, and the As-P distance, found to be 4.17 Å, the As-As distance was fixed at 4.29 Å. In a previous study of $InAs_{0.5}P_{0.5}$/InP superlattice samples, the out-of-plane As-As and As-P distances were found to be much closer to each other, about 4.28 Å and 4.25 Å respectively. In our analysis, the As-P distance is 4.17 Å, close to the P-P distance in bulk InP (4.15 Å). Therefore, we could exclude the hypothesis of a fully relaxed InAsP epilayer. The P atoms contributing to EDAFS belong to the interface region, 0.5-2 monolayers, and the core of the quantum wire is essentially strained InAs. Two types of interface or a combination of both can explain the results: a) an abrupt InAs/InP interface with periodical strain strips generated in the InP buffer layer due to the interface mismatch strain; b) a corrugated InAs/InP interface with the same periodicity as the wire.

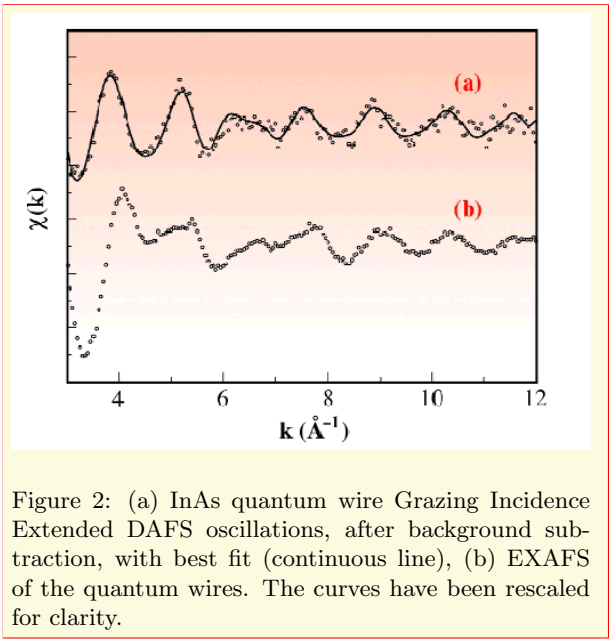

Figure 2: (a) InAs quantum wire Grazing Incidence Extended DAFS oscillations, after background subtraction, with best fit (continuous line), (b) EXAFS of the quantum wires. The curves have been rescaled for clarity.

For comparison we measured a glancing-angle EXAFS spectrum at the As K-edge (fig.2b) at beamline BM8 (GILDA, ESRF). The spectrum shows a clear As oxide shape with a strong low-frequency component that corresponds to a huge peak at 1.2 Å in its Fourier Transform (FT) (fig.3b). The oxide layer causes a significant loss of information, in particular for shells beyond the first, whereas, for a DAFS spectrum, it lowers the overall diffracted intensity and the jump at the edge, but does not perturb the fine structure signal of the interesting atoms.

For use in practical devices, the nanostructures are encapsulated or embedded in a superlattice. They must therefore be homogeneous in size, shape and composition, to provide well defined emission wavelengths. A knowledge of the strain field, chemical gradients, chemical mixing at the interface, is of great importance to understand the growth dynamics as well as the electronic and optical properties of the nanostructures.

[4] refer also to ***[2-13]*** , S. Grenier *et al.*, Eur. Phys. Lett. (2002) in Appendix for details

We have recently used GI-DAFS to study the strain, size and composition of InAs Quantum Sticks, embedded in InP ***[4-2]*** .

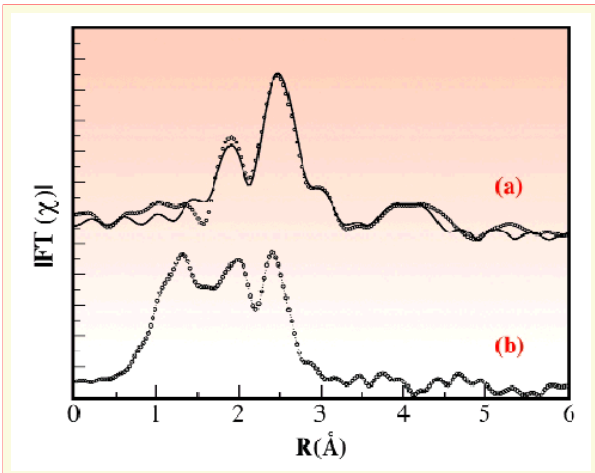

Figure 3: (a) FT of quantum wire EDAFS, with best fit (continuous curve), (b) FT of quantum wire EXAFS. The curves have been rescaled for clarity.

Compared with previous works, we used anomalous diffraction in grazing incidence at the As K-edge to study a very challenging system : nano-objects having a small size, which are encapsulated and the x-ray scattering contribution of which is mingled with that of bulk InP, whatever the momentum transfer is.
We have shown that the structure factor (i.e. the Fourier Transform) of embedded InAs stick-like nanostructures can be directly extracted, allowing the average height and strain of the QSs to be determined, their composition to be defined and the As/P exchange to be checked. GI-DAFS oscillations, in the energy range above the edge, also give direct information on the local composition and on strain accomodation inside the sticks.

In conclusion, the above results clearly show that grazing incidence anomalous diffraction and GI-DAFS are powerful tools for studying nanostructures. It is of a great importance to be able to carry out 2D anomalous diffraction mappings and GI-DAFS measurements together on a dedicated beamline with a high beam stability, such as D2AM. However, an optics update (the beamline is 10 years old), i.e., polishing the mirrors and improving the sagittal focusing of the second monochromator crystal must be carried out if the development of GI-DAFS is to be pursued. The diffractometer must also be adapted for surface scattering.

2.2 Applications of anomalous scattering at wide angles

This topic has been the subject of a general review, "Resonant Diffraction" by *J.L. Hodeau (Grenoble)* ***[1-18]*** . The notoriety of this research team has attracted many experiments on this topic, working in close collaboration on the beamline. The tunability of the beamline has also been used to characterize liquid systems and amorphous materials. Anomalous scattering of these systems seems to be the way to characterize the atomic distribution at the level of accuracy needed to validate models. *S. Hosokawa (Marburg)* began his experiments on the beamline on Ge-Se liquids ***[3-19, 3-20, 2-16, 2-17, 1-19]*** . He observed a modification in the local ordering which has been associated with a transition. He is now investigating glassy ternary alloys with As-Se.

Following some real time investigations of the recrystallisation of refractive oxides, a careful investigation of molten Y_2O_3 at high temperature was performed by *L. Hennet and coll. (Orléans)* ***[E-1, 3-16, 3-17]*** [5] To preserve the oxide from contamination, it was levitated in a gas flow while being heated by a laser. The local structure observed is close to those of the high temperature H-phase with 7 Y-O and 11 Y-Y bounds.

Single crystals

In a single crystal sample, *V. Favre-Nicolin (Grenoble)* uses the anomalous x-ray diffraction technique at the Ta L_3 edge to investigate the nature of the tantalum displacement pattern in the modulated phase of the charge-density-wave compound $(TaSe_4)_2I$ ***[E-5, 1-11]*** [6] . In addition to the known acoustic-like modulation, they find the first direct evidence for the condensa-

[5] refer to [3-16], L. Hennet *et al.*, Apl. Phys. Lett (2003) in Appendix for details
[6] refer to V. Favre-Nicolin and coll., Phys. Rev. Lett (2001) in Appendix for details

tion of optical-like Ta displacements along the metallic chains corresponding to an LLSS pattern of long and short in-chain Ta-Ta distances (Ta-tetramerization modes). The anomalous signal allows the selection of this optical-like signal which is one order of magnitude lower than the acoustic-like one. This result justifies the model in which the interaction of the electronically coupled optical modes with long-wavelength acoustic shear modes leads to the condensation of a modulation of mixed character.

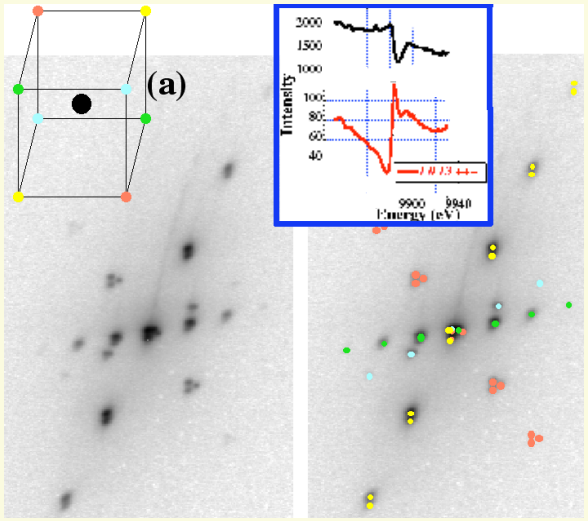

Figure 4: High-resolution image of satellite diffraction peaks, with harmonics up to 3rd order. Note the splitting of all peaks, different for all families of satellites, revealing the mono-modulation nature of each of the 4 modulated domains. An insert shows typical intensity dependence with the energy near the Ta L_3 edge of satellite peaks, which was used to characterize the optical-like modulation along the Ta chains.

Also, high-resolution diffraction at 33 *keV* (fig.4) gives insight into the domain structure, proving that each domain corresponds to a single modulation wavevector.

Multilayers.

To improve the ferroelectric properties of the $BaTiO_3$ perovskite, artificial superlattices such as $(BaTiO_3/SrTiO_3)_n$ were studied. Multilayers with artificially induced strain and chemical modulation were prepared using a CVD method and analyzed on the D2AM beamline in the thesis of *M. Nemoz (Grenoble)*. The major feature of the analysis of 00L diffraction profiles is that a unique set of parameters enables one to describe simultaneously several diffraction orders (L from 1 to 8) over 3 to 4 orders of magnitude. The fitting parameters enable us to evaluate the bilayer periodicity, the layer thickness and the thickness fluctuations, the macro-strain and the atomic intermixing at the $BaTiO_3/SrTiO_3$ interface as well as the coherence length of the stacking (Fig.5). We observe the presence of large gradients of the lattice parameter (macro-strain) and of the composition (atomic mixing) along $< 001 >$ across the interface, which dominate the diffraction curves. This significant migration of the cations throughout the bilayer is permitted by the high miscibility of Ba and Sr in all proportions in the $Ba_xSr_{1-x}TiO_3$ solid solution ***[1-4]*** .

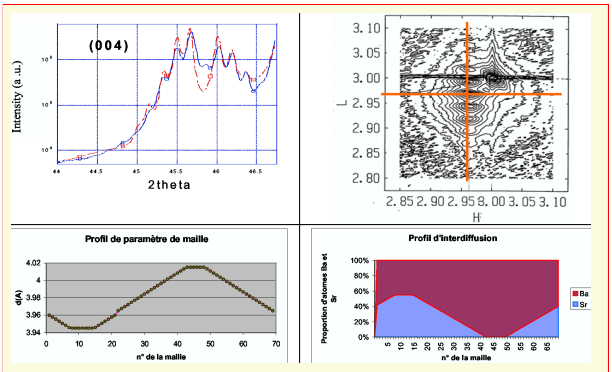

Figure 5: The HL map around the (303) peak of the same sample shows no orthorhombic distortion: $BaTiO_3$ and $SrTiO_3$ sub-layers exhibit the same a (= b) = 3.955 Å parameter, compared to a = 3.905 Å for the $SrTiO_3$ substrate. This common large in plane width of all reflections could indicate that a mirror twinned domain phenomenon occurs due to the quadratic strain induced by the $SrTiO_3$ substrate. Top left: measured (blue) and calculated (red) diffraction (004) curves of a CVD-grown multilayer composed of 15 bilayers (80 Å STO/ 80 Å BTO) at $\lambda = 0.78$ Å. Top right: HL map around the (303) peak The bottom left graph shows the variation of the lattice parameter d(001) across one bilayer. The bottom right graph shows the variation of the Ba and Sr concentration per unit cell in one bilayer.

Powder diffraction.

As a specialized powder beamline exists at the ESRF, our effort in powder applications focussed on the use of the anomalous difference to solve problems related to cation occupancy : in numerous materials cation substitution strongly modifies the properties, but conventional refinements do not allow the structural modification to be specified. This method was used in the thesis of *J. Lorimier (Dijon)* to characterize the valence distribution occurring in nanometric magnetite and complex ferrite, $Fe_{3-x}Ti_xO4$, by in-situ studies ***[T-11, 3-22, 3-24, 2-14, 1-20]*** .

In bicationic zeolite, due to the partial occupancy of the active cation site, only anomalous refinement can be used to locate cations such as Sr^{++} in one site and Br^{+} in the other. Moreover, these system are very sensitive to the reaction conditions and to approximate the catalytic process experiments must be carried in-situ.

A dedicated experimental cell was developed and tested with success during the thesis of *H. Pallancher (Grenoble)*. The quality of the data measured with this cell (fig.6) permitted the cations in Sr(Rb,Na)X zeolites to be localised on the site revealed on the Fourier map. Working near the absorption edge allows the use of the anomalous contrasts. Depending of the energy some lines increase while others decrease. Using this variation, it now possible to detail the Sr^{2+} and Rb^{+} cation distributions on the insertion sites.

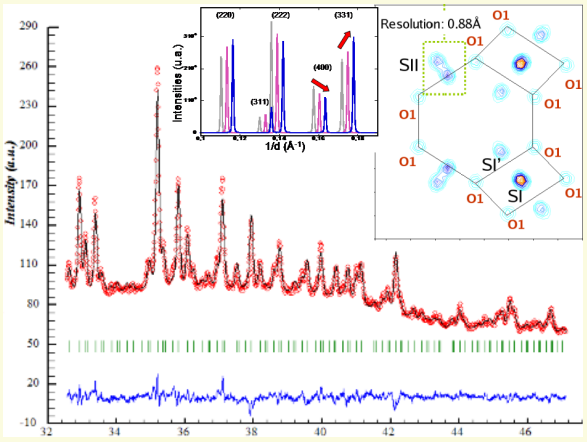

Figure 6: Part of the powder diffraction spectrum by $Sr_{25}Rb_{16}X$.
Insert : Anomalous dependence of $Sr_{25}Rb_{16}X$ diffraction lines at Sr edge and fourier map.

2.3 Diffuse scattering and weak signals

The good signal-to-noise ratio achieved on the beamline together with its harmonic purity were soon put to use by users. *M. Amara (Grenoble)* employed this set-up to detect a new quadrupolar ordering in NdMg. Superstructure peaks associated with the 4f orbital ordering were measured below the 35 K antiferromagnetic transition ***[3-1, 2-24]*** . Several days were needed to do the measurement because of the low counting rate. This success was due to the beamline stability. This set-up was also used by *S. Ravy (Orsay)* in the study of vanadium-doped blue bronze, which are quasi-one-dimensional conductors. They discovered [7] Friedel oscillations, which were predicted long ago but have remained unobserved : the pinning of the charge density wave by the defect induces an oscillation of the electron density which leads to unusual diffraction profiles for satellites ***[E-6, 2-31, 1-26]*** .

The neutral-ionic transition in mixed-stack charge-transfer organic compounds serve as a model system to study the physics of non-linear excitations. *E. Collet (Rennes)* showed that the temperature dependence of diffuse scattering is very anisotropic. He established that the evolution of certain correlation lengths agree with a one-dimensional relationship ***[E-3, E-10, H-2, 2-6]*** . There is a crossover from a 3D to a pronouced 1D regime for the fluctuations. The strong cooperativity inside the stack is reflected in the size of the strings of length about 100 Åat T_{1D}. This provides direct evidence for 1D Lattice-Relaxed Charge-Transfer fluctuations.

The signal-to-noise ratio efficiency of the beamline was also of great advantage for the study of diffuse scattering of quasi crystals by *M. de Boissieu (Grenoble)* for the thesis of *A. Letoublon* and *S. Francoual* .

[7] S. Ravy *et al.* Phys. Rev. B, 62 R16231 (2000)

Diffuse scatering of quasicrystals and phasons [8].

Quasicrystals are a new paradigm for long range order: their diffraction pattern displays sharp Bragg peaks but with a symmetry that is incompatible with translational symmetry. Their atomic structure is now better understood but the details of the structure remain to be determined. Such details are important for the understanding of physical properties of quasicrystals, but also to get some clues on their formation and stabilising mechanisms, a question which is still open. In particular, some models predict that phason fluctuations play a key role. Phason modes are collective diffusive excitations, characteristic of the long range quasiperiodic order. They lead to diffuse scattering in a way that is similar to thermal diffuse scattering. Experimentally it has been shown that the diffraction pattern of the i-AlPdMn quasicrystal displays a fair amount of diffuse scattering which can be reproduced using the generalised elasticity of quasicrystals and long-wavelength phason fluctuations. Absolute scale measurements of the diffuse scattering carried out on the D2AM beam line allowed the determination of the corresponding 2 phason elastic constants. Similar measurements have been carried out on other quasicrystals, in particular the recently discovered binary CdYb icosahedral phase. A systematic exploration of reciprocal space reveals diffuse scattering around the Bragg reflections, with characteristic anisotropies. The diffuse scattering is also due to phason fluctuations in this quasicrystal, although the phason elastic constants have not been yet determined. A comparison on an absolute scale showed that the amount of diffuse scattering is of the same order of magnitude in both the i-CdYb, the i-AlPdMn and i-AlPdRe phases (fig.8). This may be related to entropy stabilisation of these quasicrystals.

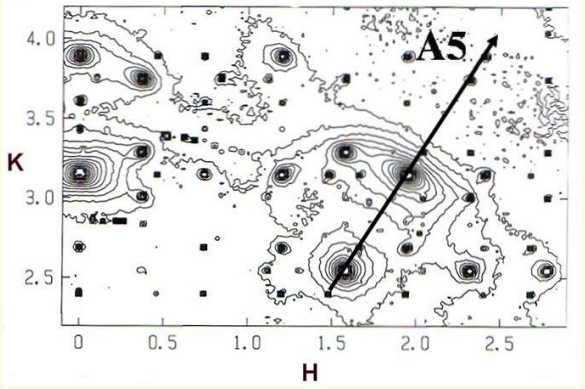

Figure 7: 2D diffuse scattering intensity distribution in the i-CdYb phase. The diffracting plane contains two orthogonal 2-fold axes (H, K), a 5-fold (A5) and a 3-fold one. The diffuse scattering exhibits different shapes around different Bragg peaks.

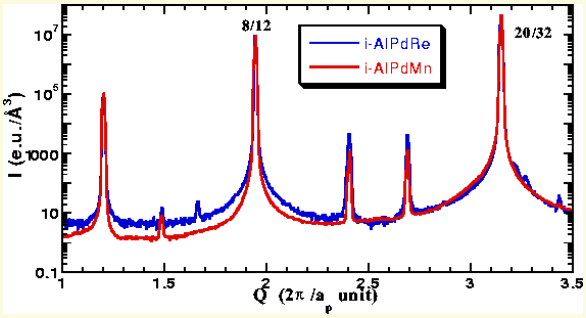

Figure 8: Absolute scale intensity of the diffuse scattering in the i-AlPdMn and i-AlPdRe quasicrystal measured along a 2-fold axis. The amount of diffuse scattering is very similar in both phases. Note the large dynamic range necessary to measure the diffuse scattering, reaching 7 orders of magnitude.

Main authors : M. de Boissieu, A. Létoublon, S. Francoual (Grenoble), A.P. Tsai, H. Takakura (Japan)
Related publications : ***[T15, H-4, 3-13, 2-7, 2-11, 1-21]***

2.4 High resolution and Coherent scattering at BM2

The source in an ESRF bending magnet is of high quality: its size is about $30\times70\ \mu m^2$ ($v\times h$, rms), and its movement is limited to a few micrometers. *F. Livet et al., (Grenoble)*, after a careful reexamination of the the characteristics of the beamline, was able to enhance the quality of the focussing and the stability of the optics of BM2. This improvement makes possible high resolution and even coherent scattering experiments. The corresponding loss of intensity was partly compensated by the use of a Direct Illumination (DI) CCD, which provides pixels of size $20\mu m$ that can be used as photon counters, with an efficiency of 50% at 7.8 KeV [9] .

[8] details in annexed publication [3-16](Letoublon et al.)
[9] *F. Livet et al.* NIM A 451, 596-609 (2000)

Large scale fluctuations in a critical system

The dynamics of the size increase of antiphase domains below T_c in $AuAgZn_2$ has been observed [10]. The high resolution of the experiment and the use of our DI CCD enabled domain sizes from 0.1 to 0.5 μm to be observed. The classical $t^{1/2}$ dependence for the domain size was verified.

Fluctuations close to the second-order ordering transition of the $AuAgZn_2$ alloy were carefully studied for a wide range of correlation lengths, from 100Å to 1000Å. Fig.9a shows the domain of q-vectors and of intensities that could be measured with our DI CCD, when the temperature is varied from T_c + 14 to T_c + 0.08 K. In the corresponding q-range, the critical slowing-down could be observed from the increase in critical fluctuation times after quenching the sample to a few tenths of K above T_c (fig.9b). This is one of the first direct observations of critical slowing down.

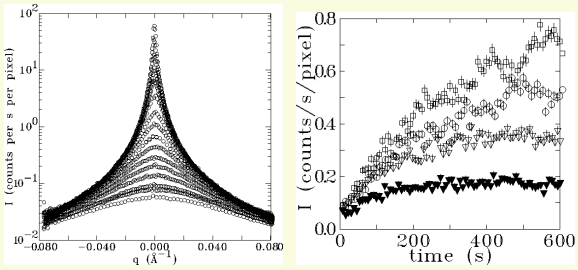

Figure 9: a : Critical scattering observed in the $AuAgZn_2$ ordering sample (from T_c + 14K to T_c + 0.08K) in the vicinity of the superstructure peak. b: Time evolution of the diffuse intensity at the superstructure peak position after quenches at $T_c + 0.13$, $T_c + 0.23$, $T_c + 0.33$ and $T_c + 0.43\,K$

Coherent scattering

Coherent scattering is observed when the resolution approaches the diffraction limit: ϵ being the rms beam divergence, and σ the rms size at the sample: $\epsilon \times \sigma \simeq \lambda$. This is easily observed with a collimated beam. Fig.10a shows diffraction of $1\mu m$ asymmetrical slits, with carefully polished edges. This development ***[3-21]*** was introduced to allow SAXS experiments to be extended to very low q-values (to $q = 4 \times 10^{-4}$Å^{-1}).

The SAXS setup was modified in order to do X-ray Photon Correlation Scattering (XPCS) in filled polymer systems ***[E-8]*** [11] These systems were filled with fumed silica particles or carbon black, and the diffusion process studied was very slow. Although our coherent beam intensity was low, of the order of 10^6 ph/s, the long time fluctuations could be observed. As a CCD was used, we obtained the characteristic times over a wide q-range: from 10^{-2}Å^{-1} to 5×10^{-4}Å^{-1}. Results from the lower q-values were compared with dynamic light scattering. The long term stability of the SAXS setup was essential for these results (see next Section for details of this experiment).

We are now able to obtain X-ray beams having a high degree of coherence, and are aiming to take full advantage of the focussing optics so as to concentrate a large coherent X-ray intensity on small crystals. Fig.10b shows the diffraction of a sub-micrometric Au crystal. This diffraction is obtained in the neighbourhood of a 111 Bragg peak, and the oscillating streaks observed correspond to facets of the crystal.

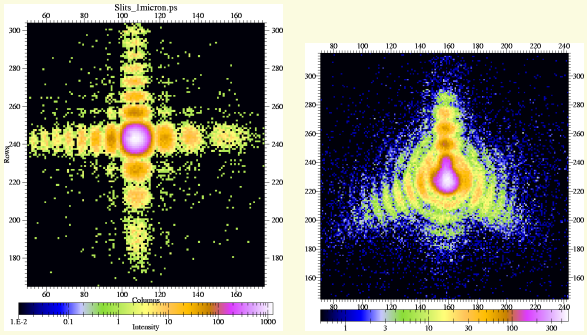

Figure 10: Left : diffraction from a square asymmetrical slit ($1 \times 1\mu m^2$). Right : scattering from a submicronic gold crystal slightly away from 111 Bragg peak center

2.5 Soft condensed matter

This heading includes not only polymers but also other disordered materials, for whose investigation the resources of D2AM proved invaluable. The accompanying articles published in Langmuir show an application of SAXS to partially ordered nanostructured materials (Ehrburger-Dolle et al.). László et al. illustrates the extended q range (more than 3 orders of magnitude) covered by D2AM and provides an example of the use of a contrast modifying medium in SAXS. The D2AM camera was also used to investigate silica glasses ***[T7, 2-20, 2-22]*** as well as solubilisation mechanisms in critical water ***[T3, H3, 3-73]*** .

[10] refer to ***[2-23]*** , F. Livet *et al.*, Phys. Rev. B (2002) in Appendix for details
[11] see also E. Geissler. *et al.* Phys. Rev. E 62 (2000) 8308-16

Distribution of divalent ions around a polyelectrolyte chain

Swollen polyelectrolyte gels, when surrounded by aqueous solutions of a monovalent salt, undergo a volume transition when divalent ions above a certain threshold concentration are added to the solution. The distribution of divalent ions in this case is not known either theoretically or experimentally. The aim of this anomalous small angle X-ray scattering study was to determine whether the divalent ions form a cloud around the polymer chain, or whether they condense on it ***[3-26]*** . The gel consisted of sodium polyacrylate in close to its volume transition, with strontium as the divalent ion. At the five different energies of the incident beam used to vary the contrast in the vicinity of $16keV$, the scattering curves have similar shapes, being separated only by constant multiplying factors (fig.11). This result, in conjunction with the SANS results from the same sample, indicates that the divalent ion (strontium) does not form an extended cloud but instead espouses the polymer backbone.

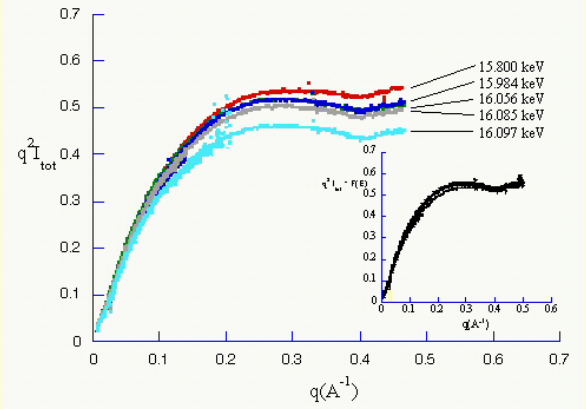

Figure 11: Kratky plot of signal from poly(sodium acrylate) gel in the presence of strontium at different energies close to the absorption edge (16.104 keV). Inset: same scattering functions normalized by the theoretical contrast factor for the strontium ions condensed on the polymer chain

Dynamics of flocculation in filled polymer melts

In the manufacture of rubbers, e.g. for automobile tyres, finely divided fillers (carbon black, silica) are blended with uncross-linked polymer. Owing to their poor solubility in this medium, the filler particles flocculate during the period before vulcanisation, an aging process that alters the elastic properties of the final product. This phenomenon was investigated by small angle coherent X-ray scattering on D2AM, in conjunction with small angle dynamic light scattering, by studying the motion of fumed silica aggregates suspended in a polymer melt, poly(dimethyl siloxane) (PDMS) ***[2-12]*** . (This topic is touched on briefly in Section 2.4 above.) The sample, in which the uncoated surface of the silica particles was hydrophilic, took the form of a high viscosity liquid (500 Pa s). The measured relaxation rates varied with the transfer wavevector q more weakly than q^2. The observed motion was found to be a combination of liquid-like diffusion in addition to a structural relaxation in which the diffusing silica aggregates recombine into larger agglomerates at long times. It obeys an equation of the form

$\Gamma = Dq^2[1 + a \times exp(-D_{SR}q^2t_0)]$

where t_0 is the time delay after the mechanical disturbance of mixing the sample into the holder. Both relaxation processes are diffusive (i.e., follow a q^2 behaviour), with rate coefficients $D = 5 \times 10^{-14}$ cm^{2}s^{-1} and $D_{SR} = 2 \times 10^{-15}$ cm^{2}s^{-1} respectively. A second sample, in which the silica surface was hydrophobic, was thixotropic. In spite of its solid-like properties on a macroscopic scale, the same double diffusion mechanism was also observed, but with much slower rate constants, 2×10^{-15}cm^{2}s^{-1} and 9×10^{-16}cm^{2}s^{-1} respectively. The differences between the samples are a consequence of the different structures of the polymer that develop around the hydrophilic or hydrophobic silica surfaces. Measurement by XPCS reduces the characteristic time constants of the relaxation processes from months on a macroscopic scale to minutes, owing to the high values of q attainable with SAXS.

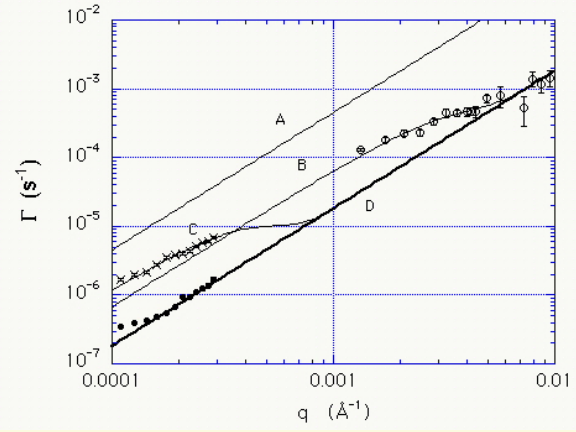

Figure 12: Relaxation rates Γ of fumed silica suspension in PDMS melt. High q: XPCS, $t_0 = 1\ h$. Low q: small angle dynamic light scattering $\times$ 10 days, . 14 days. Line D is relaxation curve for undisturbed sample. Lines B and C are calculated from the equation for the given values of t_0 .

Filler networks in elastomers

Elastomers are soft materials that can be reinforced by dispersing into them solid particles or particle aggregates such as silica or carbon black. However, the mechanism of reinforcement is still not fully understood. Our work consists in investigating by ultra small-angle X-ray scattering (USAXS) the structure of the aggregate network permeating the matrix in the initial sample and its modification during and after elongation. The goal is to relate the macroscopic mechanical behaviour with the structure of the aggregate network.

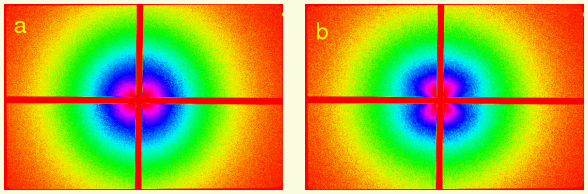

Figure 13: SAXS patterns from an uncross-linked EPR matrix filled 20 vol% of carbon black N330: unstretched (a) and vertically stretched (b). Vertical and horizontal bands are the cross-wire beamstop

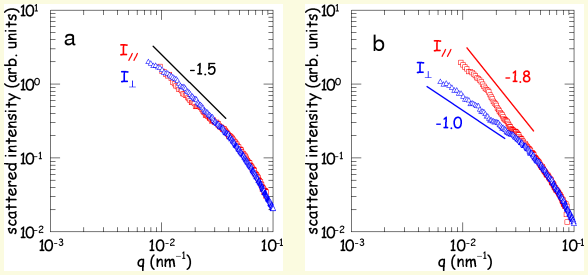

Figure 14: SAXS curves from averages over 30° sectors parallel and perpendicular to stretching axis.

For an uncross-linked EPR matrix (fig.13), the scattering pattern is isotropic both for the initial unstrained sample and for small strains. For $\epsilon > 0.20$, a characteristic "butterfly" shape appears (fig.13a). In this case, the SAXS intensity curves measured along the direction parallel ($I_{\|}$) and perpendicular ($I_{\perp}$) to the stretch axis (fig.14 b) are no longer identical, unlike undeformed or weakly elongated samples (fig.14a). The power law domain observed in a log-log plot of $I(q)$ comes from the structure factor of CB fractal aggregates ($D_f \cong 1.8$). The value of the slope is close to -1.8 for dilute dispersions. The slightly lower absolute value (1.5) measured for the initial uncross-linked sample (fig.13a) indicates that CB aggregates form a slightly interpenetrating connected networks. For $\epsilon = 0.53$, the aggregates interpenetrate strongly in the perpendicular direction (compaction).

In the direction of elongation, $I(q)$ resembles that for isolated CB aggregates, suggesting that CB aggregates become less interpenetrated along the stretch direction. The SAXS patterns measured for the cross-linked system (Fig.15) display no anisotropy for similar elongations.

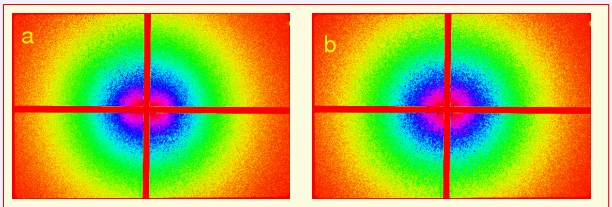

Figure 15: SAXS patterns from a cross-linked EPR matrix filled 20 vol% of carbon black N330: unstretched (a) and vertically stretched (b).

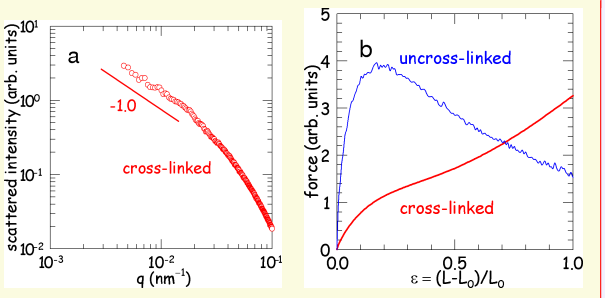

Figure 16: (a) Typical SAXS curve obtained by radial averaging for the unstretched and stretched composite. (b) Typical stress-strain curve obtained for cross-linked filled EPR matrices (unstretched and stretched).

A similar feature is also observed for concentrations below the percolation threshold, in uncross-linked EPR. Fig.16b) shows that cross-linking of the matrix induces strong interpenetration of the CB aggregates, thus forming large agglomerates. The mechanical behaviour of the two series of composites (Fig.16b) is significantly different. The shape of the curve obtained for the uncross-linked system is characteristic of a hard material in which the stiffness results from a network of slightly interpenetrating CB aggregates. The appearance of the butterfly pattern that characterises the start of the disruption of the aggregate network coincides with the maximum of the stress-strain curve. In the same strain range, cross-linked systems display no maximum. Both SAXS and mechanical measurements on cross-linked EPR thus suggest that CB aggregates may be arranged into large agglomerates separated by a layer of polymer. This hypothesis will be checked by electrical conductivity measurements.

Authors : F. Ehrburger-Dolle, F. Bley, E. Geissler, F. Livet, I. Morfin, C. Rochas (Grenoble)
Related publication : ***[E-7, 3-11,1-8,1-9]***

2.6 In situ materials science and engineering

Important contributions to engineering studies of polymers have come from experiments conducted at D2AM, as described in the book for graduate students by L. David, "Introduction à la physique des polymères" ***[2-10]*** . Metallurgical engineering has also made significant contributions using in-situ investigations.

Small-Angle Scattering for the study of precipitation in structural materials : in-situ measurements and microstructure mapping.

Structural materials, particularly those used in the transport industry, are constantly confronted with the challenge of improving their specific mechanical properties in order to achieve weight reduction. In the aerospace and automotive industry, aluminium-based alloys are widely used, and frequently gain their mechanical properties through a fine dispersion of precipitates of a second phase. The mechanical strength of these materials depends critically on the details of this dispersion, in terms of size (usually a few nm) and volume fraction (1-5 vol%), which in turn depend on the details of the temperature history that the sample has been subjected to. Small Angle Scattering proves to be the only tool that can access systematically these two parameters of the microstructure, both with good statistics and high precision.

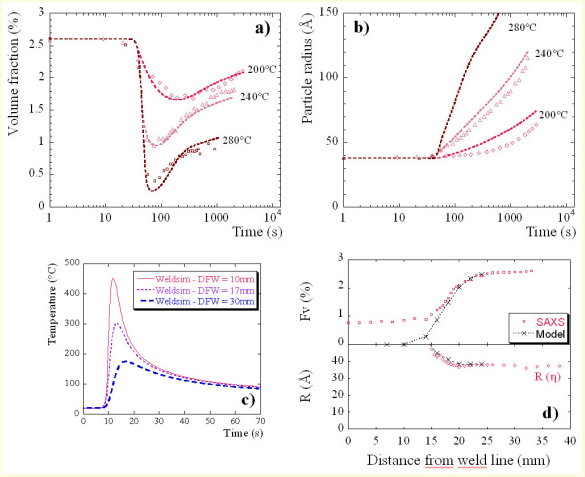

Figure 17: (a) initial state (b) evolution of volume fraction as a function of time and temperature (symbols : experiments, lines : model) (c) id., precipitate size (d) temperature cycles in a weld experienced in various points of the HAZ (e) comparison between the precipitate microstructure mapped by SAXS across the HAZ and that predicted by the precipitation model

Specific to synchrotron radiation source in terms of SAXS measurements is the reduced time of measurement (as low as 1s), which enables high quality in-situ measurements to be performed, as a function either of temperature or of deformation. This reduced time for measurement, associated with a small beam size (200 μm) also gives access to mapping of precipitate size and fraction in materials that show a microstructure gradient. This is the case notably in welding, during which the heat generated by the process affects the precipitates located in the so-called heat-affected zone. Such mapping, related to local temperature cycles, are crucial steps in optimising the welding process and in designing new alloys specifically for their welding capacity.

Figure 1 shows the dissolution behaviour of an Al-Zn-Mg alloy for automotive applications (AA7108.50). This material initially contains precipitates of radius 40$\AA$ and 2.6% in volume fraction. When subjected to a temperature rise, many of these precipitates become unstable and dissolve. However, upon dissolution (i.e., increasing solid solution), the stability of the surviving particles is increased. After a well defined minimum in volume fraction, the surviving particles start to coarsen, and the volume fraction reaches its equilibrium value at the heat treatment temperature. This behaviour can be well described by a precipitation model (dashed lines), which is a powerful tool for describing the precipitate microstructures after complicated temperature cycles such as are met in welds. Fig.17d shows such temperature cycles in the case of MIG (Metal Inert Gas) welding, as a function of the distance from the weld line. Fig.17e finally shows the comparison of a precipitate microstructural profile performed by SAXS and the model, calibrated on the reversion experiments, and applied to these temperature cycles.

continued on next page

continued from previous page

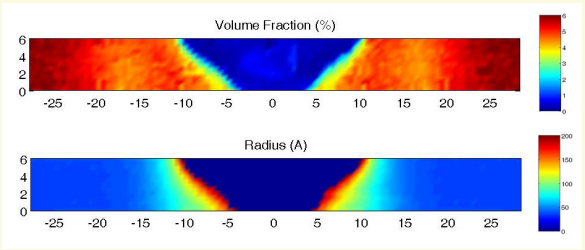

Figure 18: maps of volume fraction and size of precipitates in the plane normal to the welding direction of a friction stir welded plate of 7449 aluminium alloy. Precipitate size is initially 4 nm, and coarsens in the thermomechanically affected zone up to 20 nm. Volume fraction is initially 6 %, decreasing to 0 in the weld nugget.

Fig.18 shows the mapping of precipitate microstructures in a more complicated case, which is Friction Stir Welding (FSW) of a high strength aerospace alloy (aluminium alloy 7449). FSW is a fast-developing solid-state welding technique, involving a high temperature input and large strain deformation. Again, optimisation of the materials used and of the welding parameters needs a detailed understanding of the resulting microstructures. Precipitate size and volume fraction have been mapped in the plane normal to the welding direction ; the area where precipitate coarsening has occurred appears clearly, as well as the area of precipitate dissolution. *Main authors : A. Deschamps, F. Bley, F. Livet, J.P. Simon, M. Nicolas, F. Perrard, C. Genevois (Grenoble)*
Related publication : ***[T-6, H-1, 3-2, 3-8, 3-9, 2-27, 1-22]***

Structure and mechanical properties of Nylon fibers reinforced with nanofillers.

It is well known that inorganic nanofillers provide efficient reinforcing effects in bulk thermoplastic polymers, mainly due to their high specific surface area, which ensures strong polymer-filler interactions. Multifunctional globular polymeric particles are also nanofillers with a three-dimensional structure and numerous terminal functions. Both kinds of nanofillers are added to nylon PA6 to improve the mechanical properties of spun-drawn fibers. Structural characterisation of unfilled fibers PA6, PA6 filled with 5% globular molecules (GM) and PA6 filled with 1% of surface treated montmorillonite particles was obtained by SAXS and WAXS as a function of draw ratio.
The WAXS patterns of three kinds of spun fibers (Figure 19) display differences in crystalline structure and orientation. The majority phase of the unfilled PA6 fiber is γ (a). The PA6-clay fiber (c), also in majority in γ form, displays stronger crystal orientation parallel to the draw axis. The PA6-GM fiber (b) exhibits the presence of the crystalline α form in addition to the γ form:

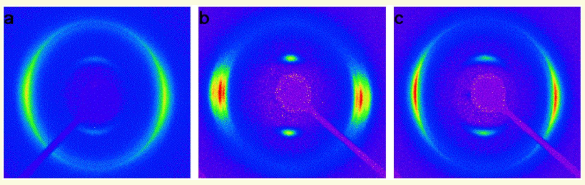

Figure 19:

Orientation is stronger for the filled PA6 fibers than for the neat PA6 fibers. The filler-matrix interactions in the melt therefore change both the rheological properties of the molten material and the crystallisation kinetics. For PA6-GM, these interactions are probably responsible for the occurrence of a significant amount of α phase, with an extended-chain conformation. The appearance of the sole γ phase in PA6-clay fiber suggests that the inorganic filler has a γ nucleating effect, as reported for bulk crystallised PA6. The presence of fillers also affects the fibrillar structure as shown in the following SAXS patterns (Figure 20)), which display strong anisotropy with lobes:

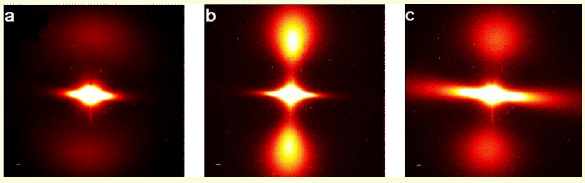

Figure 20:

From the projection along the fiber axis, the long period, L_p, lamellar crystal thickness, L_c, and amorphous layer thickness, were estimated A transverse analysis of the SAXS lobes gives access to the fibril radius.

continued on next page

continued from previous page

The intensity of the meridian lobes characteristic of the periodic amorphous-crystal arrangement of the fibrillar structure is strongly increased in the case of the as-spun filled fibers. The fibril radius increases with increasing filler content. The strong equatorial scattering of the clay-PA6 fiber (c) is due to the alignment of the clay platelets parallel to the fiber (draw) axis. Stretching the fibrils during the initial stage of drawing first involves an increase of the long period at secondly a decrease of the fibril diameter. Then, the slippage of the fibrils past each other involves peeling off the fibrils by chain unfolding from the lateral surfaces.

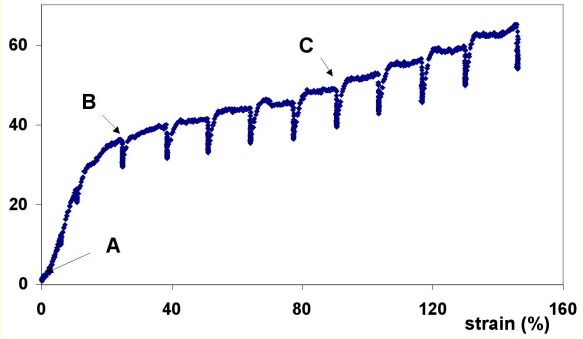

Figure 21: Relaxation during elongation. Spikes are the relaxation after a SAXS measurement at constant strain.

The SAXS pictures obtained for PA6 during elongation at points A, B and C were very different:

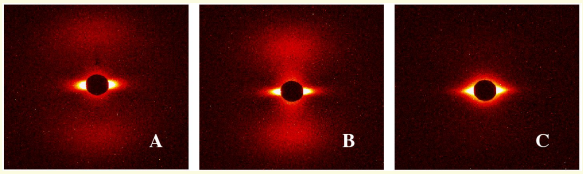

Figure 22:

As strain is increased (from A to C), the meridional lobes move toward the beamstop, indicating that the long period increases.
The crystalline structure and the fibrillar morphology of spun PA6 fibers are sensitive to the presence of nanofillers. Stretching of the fibrils followed by slippage is observed at a microscopic scale for all kinds of fibers, except at the maximum draw ratio. The mechanical properties of drawn fibers are also sensitive to the presence of nanofillers. The filler reinforcement can be explained if filler particles are unable to fit into the amorphous intrafibrillar regions, and are absent in the interfibrillar regions. Stiffness reinforcement of the PA6-GM fibers can thus be ascribed to reduced interfibrillar slip in the fibers due to a physical crosslinking effect. In the case of the clay-filled fibers, mechanical improvement is less pronounced at equivalent draw ratio.
Main authors : C. Ibanes, R. Seguela , L. David (Lyon) C. Rochas , M. De Boissieu, (Grenoble), G. Robert (Rhodia)
Submitted for publication, J. Polymer Science
Related publication : ***[T-2, 2-19]***

2.7 Detector development

Currently available 2D detectors do not make full use of the high flux and high brilliance of third generation synchrotron sources. For this reason numerous experiments are still performed using slits and photomultipliers that allow only point detection. At the present time, the detectors in most common use are CCD cameras with indirect photon detection.

Modern CCD detectors exceed 10^6 pixels and their reading-time is close to a second. They are suited for structure collection as integrating devices. The dark current and the converter noise amount to a few counts on a maximum scale of 16 bits. Their complex optical system degrades the properties of the incoming photons: low counts no longer obey a Poisson distribution and the spatial transfer function produces tails that preclude measurements of weak signals near a peak that may spill over its neighbouring pixels. Moreover, they require a cooling system to reduce the dark current as well as the use of a mechanical shutter.

Active pixel detectors have been developed for high energy physics, they present a new opportunity to improve the quality of our measurements.

The XPAD project

The XPAD project is headed by CPPM-IN2P3 (Marseille), LdC (Grenoble) and the CRG-D2AM beamline.

The XPAD photon counting detector, suitable for materials science and small angle scattering experiments similar to those performed on D2AM, should have the following characteristics : wide dynamic range ($> 10^9 photons/pixel$), saturation rate up to $10^7 ph/s/pixel$ and a noise lower than $0.1 ph/s/pixel$. In our detector, incoming photons are converted to an electron cloud in the sensor in which a polarization ensures migration of the charge through the bump to the electronic chip. In each pixel, the electron bunches are then treated by dedicated electronics. By virtue of this wide parallelism, very short reading times can be achieved (less than 1ms). On-board memories allow frames for real time kinetics experiments to be stored ***[E-4, 3-5, 2-4, 2-5, 2-8]*** .

The prototype

The XPAD prototype, with pixel size $330 \times 330 \mu m^2$, was manufactured by AMS with $0.8 \mu m$ CMOS technology. The most sensitive part of the design was the analog block, owing to the conflicting requirements of high counting rate and high sensitivity. At 20keV, a photon produces 5500 electrons but only 1400 at 5 keV. These charges must be discriminated from the noise. In each pixel, the discriminator has to be adjusted independently because of the fluctuations in component values generated by the different processing steps.

Each pixel response can be measured with a charge injector to allow pre-configuration of the detector. At the discriminator exit, a logical gate enables counting for the desired acquisition time and, if necessary, can switch off a damaged pixel. This block is followed by a 16 bit counter located in each pixel. A common logical unit located at the bottom of the chip ensures the interface with the outside world : dialogue, timing, ... The chips are then mounted on an epoxy card together with a few elements and an ALTERA programmable chip to handle dialogue and control the memory for the external counters. All this is then monitored by a PC for the test acquisitions.

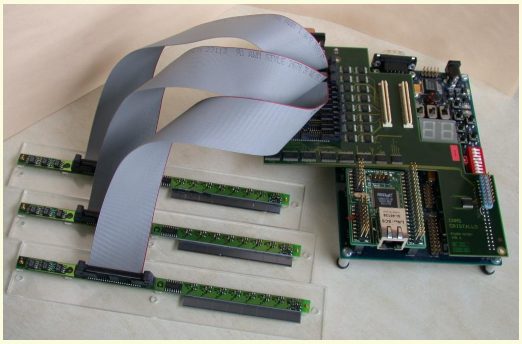

Figure 23: 3 modules of 8 chips connected to the acquisition card.

Results

Electronic tests in the lab show that the pulse width at the amplifier output was about $0.1 \mu s$, which is close to the expected value needed to reach the design counting rate. The configuration of the chips was carried out using a radioactive source and an X-ray tube. These preliminary tests exhibited a broad dispersion in the characteristics of the threshold level of the pixels. It revealed the difficulties for finding a configuration in which more than 90% can be simultaneously tuned.

Tests were then performed with the the detector mounted on the D2AM SAXS station so as to define a very small and clean incident beam. The energy response of detector was tested between 10 and 24 keV. The energy resolution is estimated to be about 1 keV. A charge spread of $60 \mu m$ was measured by scanning the detector with a very narrow beam $10 \times 50 \mu m^2$. It can be reduced by setting the threshold level at exactly half of the incoming energy : in this case, whatever is the division, the photon is detected by one only of the pixels. The dynamic range was also checked : the xpad pixel detector measures counts ranging from $.01 ph/s/pixel$ to $2.510^6 ph/s/pixel$. At high count rates when the pixel saturated, no influence could be detected on adjacent pixels.

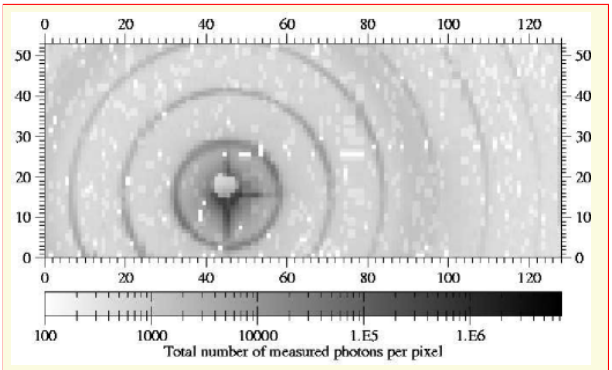

Figure 24: SAXS on Silver Behenate : up to 7 orders of diffraction have been recorded as well as intensities close to the direct beam

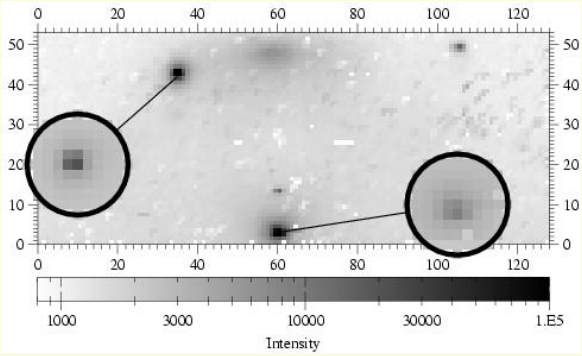

Figure 25: Bragg peaks and diffuse scattering of CdYb quasicrystal. Inserts are zooms using a gray scale shifted by 2 orders of magnitude.

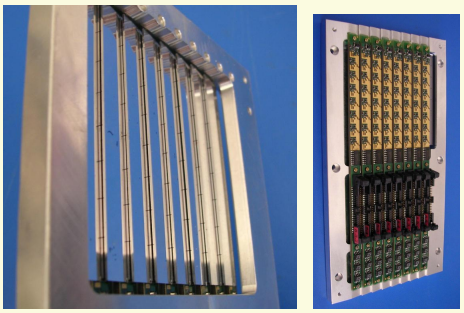

Figure 26: Front view of the 8 modules assembly: the $500\mu m$ thick Si diodes. Rear view : the electronic chips.

The modules are tiled as close as possible to each other to reduce shading and dead zones as illustrated bellow. The detector size is 200×192 pixels, which gives a surface of about $68 \times 68 mm^2$.

In conclusion, pixel detectors can attain the performances needed for high dynamic studies. This is illustrated by the SAXS pattern of silver behenate (a standard for SAXS experiments, d=58,38 Å) and CdYb icosahedral quasicrystal Bragg peaks and diffuse scattering shown below. These images were measured at 20 keV, on a continuous diode bumped to 2 rows of 5 chips. White pixels are those for which the tuning is out of range. The number of truly dead pixel is fewer than 2 %.

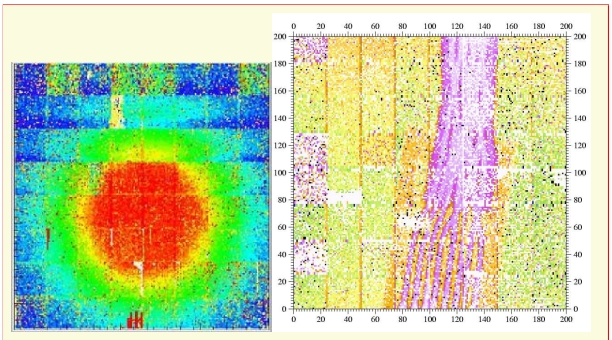

Figure 27: Right : raw image of a radioactive source as delivery test of the assembly.
Left : uncorrected test image of a network plug: orange lines count less due to shading.

Future developments

Our goal is to develop a real detector with more than 10^6 pixels. Such a detector will consist of several modules to be tiled together. This step has recently been validated by assembling 8 modules of 8 chips each.

To achieve the number of pixels required in numerous experiments, we have already begun the design of a new chip XPAD3. It will use radiation-hard submicronic technology (0.25 microns), which will allow the pixel size to be reduced to $100 - 150\mu m$ with similar or enhanced performance.

Appendices

Selected reprints accompanying this report

EUROPHYSICS LETTERS 15 February 2002

Europhys. Lett., **57** (4), pp. 499–505 (2002)

Grazing-incidence diffraction anomalous fine structure of InAs/InP(001) self-assembled quantum wires

S. Grenier[1], M. G. Proietti[2], H. Renevier[1], L. González[3], J. M. García[3] and J. García[2]

[1] *Laboratoire de Cristallographie, CNRS - B.P. 166, 38042 Grenoble Cedex 09, France*
[2] *Departamento de Física de la Materia Condensada, Instituto de Ciencia de Materiales de Aragón, CSIC-Universidad de Zaragoza - c. Pedro Cerbuna 12, 50009 Zaragoza, Spain*
[3] *Instituto de Microelectrónica de Madrid, CSIC c. Isaac Newton 8, 28760 Tres Cantos, Spain*

(received 29 May 2001; accepted in final form 20 November 2001)

PACS. 61.10.-i – X-ray diffraction and scattering.
PACS. 61.10.Ht – X-ray absorption spectroscopy: EXAFS, NEXAFS, XANES, etc.
PACS. 68.65.-k – Low-dimensional, mesoscopic, and nanoscale systems: structure and non-electronic properties.

Abstract. – We have studied nanostructured samples of InAs/InP(001) by means of Grazing Incidence Diffraction Anomalous Fine Structure. The samples, grown by molecular beam epitaxy, show a periodic corrugation on the surface giving rise to an array of self-assembled quantum wires after deposition of 2.5 monolayers of InAs. We measured the (440) and (420) GIDAFS spectra, at the As K-edge, at incidence and outgoing angles close to the substrate's critical angle. We analysed the anomalous diffraction lineshapes *vs.* the energy, as well as the oscillatory part of the signal in the extended region above the edge and obtained, for the first time, information about composition and strain *inside* the quantum wires and *close* to the interface. Our results suggest possible interfaces.

APPLIED PHYSICS LETTERS VOLUME 83, NUMBER 16 20 OCTOBER 2003

Melting behavior of levitated Y_2O_3

L. Hennet, D. Thiaudière, C. Landron, P. Melin, and D. L. Price[a)]
CRMHT, 1d avenue de la Recherche Scientifique, 45071 Orléans Cedex 2, France

J.-P. Coutures
IMP, Rambla de la Thermodynamique, 66100 Perpignan, France

J.-F. Bérar
LCG, 25 avenue des Martyrs, 38042 Grenoble Cedex 9, France

M.-L. Saboungi
CRMD, 1bis rue de la Férollerie, 45071 Orléans Cedex 2, France

(Received 18 June 2003; accepted 29 August 2003)

The yttrium environment in liquid Y_2O_3 at 2770 K has been measured with anomalous x-ray scattering, aerodynamic levitation, and laser heating. The Y–O coordination of 6–7 and the Y–Y coordination of around 12 imply that the close packing of the high-temperature (H-type) solid phase is preserved on melting, in contrast to the large structural changes exhibited by Al_2O_3. The unusually sharp main diffraction peak implies a high degree of chemical order and mirrors the diffraction pattern of the H-type phase. © *2003 American Institute of Physics.*
[DOI: 10.1063/1.1621090]

Structural Evidence for Ta-Tetramerization Displacements in the Charge-Density-Wave Compound $(TaSe_4)_2I$ from X-Ray Anomalous Diffraction

V. Favre-Nicolin,[1,2] S. Bos,[1] J. E. Lorenzo,[1] J-L. Hodeau,[1] J-F. Berar,[1] P. Monceau,[3] R. Currat,[4] F. Levy,[5] and H. Berger[5]

[1]*Laboratoire de Cristallographie-CNRS, BP 166, 38042 Grenoble Cedex 9, France*
[2]*Laboratoire de Cristallographie, 24 Quai E-Ansermet, CH-1211 Geneva, Switzerland*
[3]*CRTBT-CNRS, BP 166, 38042 Grenoble Cedex 9, France*
[4]*ILL, BP 156, 38042 Grenoble Cedex 9, France*
[5]*Physics Department, EPFL, CH-1015 Lausanne, Switzerland*

(Received 28 March 2001; published 18 June 2001)

We use the anomalous x-ray diffraction technique to investigate the nature of the tantalum displacement pattern in the modulated phase of the charge-density-wave compound $(TaSe_4)_2I$. In addition to the known acousticlike modulation, we find the first direct evidence for the condensation of opticlike Ta displacements along the metallic chains corresponding to an *LLSS* pattern of long and short in-chain Ta-Ta distances (Ta-*tetramerization* modes). This result confirms a previous model in which the interaction of the electronically coupled optic modes with long-wavelength acoustic shear modes leads to the condensation of a modulation of mixed character.

DOI: 10.1103/PhysRevLett.87.015502 PACS numbers: 61.50.Ks, 61.10.–i, 64.70.Rh, 71.45.Lr

PHILOSOPHICAL MAGAZINE LETTERS, 2001, VOL. 81, NO. 4, 273–283

Phason elastic constants of the icosahedral Al–Pd–Mn phase derived from diffuse scattering measurements

A. LÉTOUBLON†, M. DE BOISSIEU†*, M. BOUDARD†, L. MANCINI‡, J. GASTALDI§, B. HENNION‖, R. CAUDRON¶ and R. BELLISSENT‖

† Laboratoire de Thermodynamique et Physico-chimie Métallurgiques, Unité Mixte de Recherche associée au CNRS 5614, Ecole Nationale Supérieure d'Electrochimie et de Electrométallurgie de Grenoble, Institut National Polytechnique de Grenoble, F-38402 St Martin d' Hères Cedex, France
‡ LAMEL, Consiglio Nazionale delle Richerche, Via Gobetti 101, 40129 Bologna, Italy
§ Centre de Recherche sur les Mécanismes de la Croissance Cristalline, CNRS, Campus de Luminy, Case 913, F-13288 Marseille Cedex 9, France
‖ Laboratoire Léon Brillouin, Centre d'Etudes Saclay, F-91191 Gif sur Yvette Cedex, France
¶ Office National d'Etudes et de Recherche Aérospatiales BP 72, F-92320, Chatillon, France

[*Received in final form 30 November 2000 and accepted 8 December 2000*]

ABSTRACT

The diffuse scattering in the diffraction pattern of the icosahedral Al–Pd–Mn quasicrystalline phase has been measured on an absolute scale by X-ray and neutron scattering on single-grain samples. Most of the diffuse scattering can be interpreted in the framework of the elasticity theory of icosahedral quasicrystals considering only phason fluctuations. At room temperature the absolute values of the K_1/k_BT and K_2/k_BT phason elastic constants are of the order of 0.06 and 0.031 atom^{-1}. The amount of diffuse scattering intensity is insensitive to the sample annealing treatment.

PHYSICAL REVIEW B **66**, 134108 (2002)

Statics and kinetics of the ordering transition in the $AuAgZn_2$ alloy

Frédéric Livet,* Françoise Bley,† and Jean-Paul Simon‡
Laboratoire de Thermodynamique et de Physico-Chimie Métallurgique (UMR CNRS 5614), ENSEEG-INPG, BP 75, 38402 Saint Martin D'Hères, France

René Caudron§
ONERA, 29Av. Div. Leclerc, 92320 Chatillon, France
and LLB, CNRS-CEA, CE Saclay, 91190 Gif sur Yvette, France

Jacques Mainville‖ and Mark Sutton¶
Physics Department, McGill University, Montreal, Québec, Canada H3A 2T8

David Lebolloc'h**
LPS, Bât. 510, Univ. Paris Sud, 91405 Orsay, France

(Received 19 April 2002; revised manuscript received 18 July 2002; published 31 October 2002)

The Heusler order-disorder transition in the $AuAgZn_2$ alloy is studied by x-ray scattering using the D2AM beamline at the ESRF. The static critical fluctuations above T_c are measured and are shown to follow Ising-like behavior. *In situ* kinetics of ordering are studied at T_Q after quenching from T_c+5 °C. For $T_Q<T_c-2$ °C, the growth of ordered domains is shown to have a $t^{1/2}$ dependence. For temperatures closer to T_c, the influence of critical fluctuations on the kinetics is discussed. First, the time increase of the fluctuations after quench above T_c is observed. The T_Q and q dependence of the process is discussed from a dynamical scaling hypothesis. For $T_c>T_Q>T_c-2$ °C, the main observation in the vicinity of T_c is the observation of an *incubation time* before the normal $t^{1/2}$ domain growth. These experiments provide direct observations of the critical slowing down in a critical system with a nonconserved order parameter.

DOI: 10.1103/PhysRevB.66.134108 PACS number(s): 64.60.Ht, 05.70.Jk, 61.10.Eq, 05.70.Fh

Langmuir **2003,** *19,* 4303−4308

Small-Angle X-ray Scattering and Electron Microscopy Investigation of Silica and Carbon Replicas with Ordered Porosity

Françoise Ehrburger-Dolle,* Isabelle Morfin, and Erik Geissler

Laboratoire de Spectrométrie Physique, UMR 5588 CNRS−UJF, Domaine Universitaire, BP 87, 38402 Saint Martin d'Hères Cedex, France

Françoise Bley and Frédéric Livet

Laboratoire de Thermodynamique et de Physico-Chimie Métallurgiques, UMR 5614 CNRS−UJF, ENSEEG−INPG, Domaine Universitaire, BP 75, 38402 Saint Martin d'Hères Cedex, France

Cathie Vix-Guterl and Seifedine Saadallah

Institut de Chimie des Surfaces et Interfaces, UPR 9069 CNRS, 15 rue Jean Starcky, BP 2488, 68057 Mulhouse Cedex, France

Julien Parmentier, Mohamad Reda, and Joël Patarin

Laboratoire des Matériaux Minéraux, UMR 7016 CNRS−UHA, Ecole Nationale Supérieure de Chimie de Mulhouse, 3 rue Alfred Werner, 68093 Mulhouse Cedex, France

Monica Iliescu and Jacques Werckmann

Institut de Physique et de Chimie des Matériaux de Strasbourg, UMR 7504 CNRS−ULP, 23 rue du Loess, 67037 Strasbourg Cedex, France

Received December 3, 2002. In Final Form: February 28, 2003

Ordered nanoporous carbons can be prepared by a replica technique starting from an organized silica template. The silica template used, SBA-15, displays hexagonal arrangements of mesopores interconnected by micropores. Two routes are possible for introducing carbon into the pores of the silica: liquid impregnation by a solution of sucrose followed by carbonization or chemical vapor infiltration (CVI). After dissolution of the silica template by hydrofluoric acid treatment, a carbon material is obtained. Small-angle X-ray scattering (SAXS) measurements were performed over a broad range of wave vector q in order to investigate the multiscale structure of the carbon replica as a function of the method of infiltration (liquid or gas route) and the amount of infiltrated carbon. Because of the close match in electron density between silica and carbon, it is possible to investigate the silica mesopore filling. It appears that at least 50% of the pore volume must be filled in order to obtain an organized carbon replica after dissolution of the silica template. It is also shown that the gas route (CVI) prevents the spatially proportional (i.e., affine) shrinkage observed for replicas prepared by liquid impregnation. TEM confirms that the organized carbon is a nearly perfect negative replica of the silica porous structure.

Langmuir **2004,** *20,* 1321−1328

Morphological Investigation of Chemically Treated Poly(ethylene terephthalate)-Based Activated Carbons

Krisztina László,*,† Katalin Marthi,‡ Cyrille Rochas,§ Françoise Ehrburger-Dolle,§ Frédéric Livet,|| and Erik Geissler§

Department of Physical Chemistry, Budapest University of Technology and Economics, H-1521 Budapest, Hungary, Research Group for Technical Analytical Chemistry, Hungarian Academy of Sciences, Department of General and Analytical Chemistry, Budapest University of Technology and Economics, H-1521 Budapest, Hungary, Laboratoire de Spectrométrie Physique UMR 5588 CNRS-Université J. Fourier de Grenoble, BP 87, 38402 St. Martin d'Hères Cedex, France, and Laboratoire de Thermodynamique et Physico-Chimie Métallurgiques UMR 5614 CNRS-Institut National Polytechnique de Grenoble, BP 75, 38402 St. Martin d'Hères Cedex, France

Received October 21, 2003. In Final Form: December 16, 2003

Complementary techniques, including low-temperature nitrogen adsorption and small-angle X-ray scattering (SAXS), are applied to detect the effects of surface functionalization on the morphology of activated carbon derived from poly(ethylene terephthalate) (PET). Scanning electron microscopy (SEM) is also employed as an auxiliary method to visualize the surface below the micron scale. The SEM images reveal a micron-sized ridgelike texture. Room temperature acid treatment makes the ridges become more pronounced, while treatment with boiling acid uncovers fiberlike structures of roughly 1 μm diameter. All samples display an apparent surface fractal dimension of $D_s = 2.4$ in the wave vector range 0.001−0.02 Å^{-1}. Nitric acid at room temperature increases the surface oxygen content only by 3 at. %, while all the adsorption properties and structural parameters reported in this paper are virtually unaffected. Significant differences in the morphology at submicron scales appear only after boiling acid treatment. The resulting carbon remains highly microporous, but the loss of Brunauer−Emmett−Teller (BET) surface area from about 1150 to 304 m^2/g is approximately 75%. In addition to the principal peak at around 8 Å, fresh peaks appear in the polydisperse Horváth−Kawazoe (HK) pore size distribution owing to the burnoff of intervening walls. The average width of the slitlike pores calculated from the Dubinin−Radushkevich (DR) plot increases from 8.4 to 11 Å. The minimum slit width where the applied probe molecules, that is, nitrogen and hexane, can enter increases from about 5 to about 5.4 Å. The separation distance of the basic structural units is practically unchanged. When, however, this carbon is in contact with hexane, this distance expands from about 19 to 27 Å. The swelling is consistent with the deformable nature of this sample also illustrated by the low-pressure hysteresis and the reduced helium density. Particular attention was paid to the surface areas derived from low-temperature nitrogen adsorption and X-ray measurements. Owing to the wide spatial range of the structures in these samples, estimates of the specific surface area of activated carbons can be substantially in error unless both upper and lower q ranges of the SAXS spectra are taken into account. Surface areas derived from the adsorption data either by the BET or the DR approaches were always below the values obtained by standard SAXS. As an example, the carbon sample functionalized at room temperature gave surface area values of 1114, 1293, and 1970 m^2/g, respectively. The possibility that this difference is caused by inaccessible pores was excluded by contrast variation measurements with hexane.

References

ESRF HighLights 2003-1999

E-1 Hennet L., D. Thiaudiere, C. Landron, J.F. Berar, M.L. Saboungi, G. Matzen, D.L. Price : *"X-ray Scattering on Molten Levitated Y_2O_3"* **2003, Material Sciences**, p 40-41

E-2 Letoublon A., V. Favre-Nicolin, H. Renevier, M.-G. Proietti, C. Monat, M. Gendry, O. Marty, C.Priester *"InAS Quantum Sticks : Determination of Strain, Size and Composition"* **2003, Surface and Interface Science**, p 71-72

E-3 Collet E., M.H. Lemee-Cailleau, M. Buron, H. Cailleau, S. Ravy, T. Luty, J.F. Berar, P. Czarnecki and N. Karl *"Direct evidence of lattice-relaxed Charge-transfer Exciton-string"* **2002, Material Sciences**, p 70-71

E-4 Bérar J.F., Blanquart L., Boudet N., Breugnon P., Caillot B., Clemens, J.C., Koudobine I., Delpierre P., Mouget C., Potheau R. and Valin I. *" A Pixel Detector with large dynamic range for high counting rates "* **2002, Industrial and Applied Research**, p 91-22

E-5 V. Favre-Nicolin, S. Bos, J. E. Lorenzo, J-L. Hodeau, J-F. Berar, P. Monceau, R. Currat, F. Levy, and H. Berger *" High-resolution Diffraction Study of the Charge-Density-Wave for the Compound $(TaSe_4)_2I$"* **2001 Collective Atom Dynamics**, p60-61

E-6 S. Ravy, S. Rouzière, J.P. Pouget, S. Brazovskii and J.F.Bé rar *"Oscillations in Quasi-one-dimensional Conductors"* **2001 Collective Atom Dynamics**, p61-62

E-7 F. Ehrburger-Dolle, M. Hindermann-Bishoff, F. Livet, F. Bley, C. Rochas, E. Geissler *"Anisotropic USAXS in Carbon Black-filled Polymers."* **2000, Soft Condensed Matter**, p 34-35

E-8 E. Geissler, A.-M. Hecht, C.Rochas, F. Bley, F. Livet, M. Sutton *"Correlation Spectroscopy on Filled Polymers and their Flocculation."* **2000, Soft Condensed Matter**,p 35-36

E-9 J. Garcia, G. Subias, M.G. Proietti, J. Blasco, H. Renevier, J.L. Hodeau, Y. Joly *"Charge Ordering and Forbidden Reflections in Magnetite."* **1999, Electronic States and Lattice Dynamics**, p 53-54

E-10 E. Collet, M. Buron-Le Cointe, M.H. Lemée-Cailleau, H. Cailleau, M. Meven, S. Mattauch, G. Heger, J.F. Bérar, N. Karl *"Neutral-Ionic Layered Ordering and Condensed Charge-Transfer Exciton-Strings in DMTTF-CA."* **1999, Electronic States and Lattice Dynamics**, p 54-55

Theses and Habilitation Degrees (2003-2000).

The following works have taken benefit from experiments carried on the beamline.

T-1 Bou-Huot Phe :*"Couplage Mise en forme et élaboration de matériaux hybrides organiques - inorganiques dans les procédés d'extrusion, d'injection et d'enduction (EVA/Silice)."* **thesis 2003**, INSA Lyon

T-2 Cécile Ibanes :*"Relations Structure- Propriétés mé caniques de fibres de polyamide 6 renforcées de nanoparticules organiques ou minérales."* **thesis 15 Oct 2003**, INSA Lyon

T-3 Denis Testemale :*"Structures locales en solution aqueuse supercritique."* **thesis 3 Oct 2003**, UJF Grenoble

T-4 Rémi Pantou :*"Synthèse de couches BTO/STO par CVD à injection."* **thesis 2003**, LMGP, INPG, Grenoble

T-5 Sébastien Adora :*"Analyse XAS, XRD et HRTEM des é tapes d'élaboration de nanoparticules de platine réalisées sur carbone activé par imprégnation de H_2PtCl_6 puis réduction électrochimique."* **thesis 18 Déc. 2002**, INPG, Grenoble

T-6 Myriam Nicolas-Dumont :*"Evolution de l'état de pré cipitation dans un alliage Al-Zn-Mg lors de traitements thermiques anisothermes et dans la zone affectée thermiquement de joints soudés."* **thesis Déc. 2002**, INPG, Grenoble

T-7 Rozenn Le Parc :*"Diffusion de rayonnements et relaxation structurale dans les verres de silice et les préformes de fibres optiques."* **thesis 23 Sep. 2002**, Univ. C. Bernard, Lyon

T-8 Ovidiu Ersen :*"Etude structurale et magnétique de couches minces anisotropes a base de cobalt; étude par DAFS de la structure locale de couches épitaxiées."* **thesis 18 Déc. 2001**, Univ. L. Pasteur, Strasbourg

T-9 Stephane Grenier :*"Spectroscopie de diffraction ré sonnante - Etudes de nanostructures de semiconducteurs III-V et de l'ordre de charge dans NaV_20_5."* **thesis 9 Nov. 2001**, UJF Grenoble

T-10 David Dumont :*"Relations Microstructures/Tenacité dans les alliages aéronautiques de la série 7000"* **thesis 4 Avril 2001**, INPG Grenoble

T-11 Johan Lorimier :*"Problématique des valences mixtes dans les ferrites nanométriques : possibilités offertes par la diffraction résonnante des rayons X"* **thesis 14 Mars 2001**, Univ. Dijon

T-12 Cyril Chacon :*" Synthese, etude cristallographique et caracterisation magnetique de composes intermetalliques R-M-B a base d'elements de terre rare (R), de metaux de transition 3d (M) et de bore (B)"* **thesisDéc. 2000**, UJF Grenoble

T-13 Thierry Bigault :*"Etude des contraintes et des dé formations au cours de la croissance de couches métalliques; analyse de la structure et du profil de composition aux interfaces par diffusion des rayons X"* **thesis 6 Avril 2000**, Univ. Marseille

T-14 Gloria Subias Peruga :*"Estructura electronica y geometrica local de oxidos de valencia mixta : Magnetita y Perovskitas de manganeso"* **thesis Fev. 2000**, Univ. Zagora

T-15 Antoine Létoublon :*" Diffusion diffuse et phasons dans les phases icosaédriques et icosaédriques modulées Al-Pd-Mn"* **thesis 20 Janv. 2000**, UJF Grenoble

T-16 Regis Guillot :*""* **thesis 4 Dec. 2002**, UP Nancy

H-1 Alexis Deschamps :*"Précipitation durcissante dans les matériaux de structure"*, **DHDR, juillet 2003** , INPG Grenoble

H-2 Marie-Héelène Leme-Cailleau :*"Transitions de phase dans les cristaux moléculaires : de l'équilibre thermique sous pression vers le contrôle optique"*, **DHDR, 3 Avril 2003** , Univ. Rennes

H-3 Jean-Louis Hazemann :*"Mise en évidence des modifications structurales locales dans des solutions aqueuses en conditions sub et supercritiques"*, **DHDR, 10 Nov. 2003**, UJF Grenoble

H-4 Marc De Boissieu :*"Quasicristaux : structure atomique, phonons et phasons."*, **DHDR, Juin 2003**, UJF Grenoble

H-5 Hubert Renevier :*"Spectroscopie de Diffraction Résonante. Etudes de nanostructures et corrélations électroniques."*, **DHDR, Déc. 2001**, UJF Grenoble

M-1 Mélissa Delheusyu :*"Etude de la mise en ordre et de la démixtion dans les superalliages NiCrAl par diffusion des rayons X aux petits angles et aux grands angles sur synchrotron."* **Ingénieur Civil Physicien, Sept. 2002**, Univ. Liège

Publications 2004

4-1 Laszlo K., Marthi K., Rochas C., Ehrburger-Dolle F., Livet F., Geissler E. : *" Morphological Investigation of Chemically Treated Poly(ethylene terephthalate)-Based Activated Carbon"* **Langmuir 20** (2004) 1321-1328

4-2 Letoublon A., Favre-Nicolin V., Renevier H., Proietti M.G., Marty O., Monat C., Gendry M., Priester C. : *"Strain, size and composition onf InAS Quantum Wires, embedded in InP determined via Grazing Incidence X-ray Anomalous Diffraction"* **Phys. Rev. Lett. (2004) cond-mat0309522** accepted

4-3 Rousseau G., Desgranges L., Niepce J-C., Berar J.-F., Baldinozzi G. : *"Synchrotron Diffraction Study of the Isothermal Oxidation of Uranium Dioxide at 250° C"* **Mat. Res. Soc. Symp. Proc. Vol. 802** (2004) DD1.2.1-6

4-4 Saiani A., Rochas C., Eeckhaut G., Daunch W.A., Leenslag J.-W., Higgins J.S. : *"Origin of Multiple Melting Endotherms in a High Hard Block Content Polyurethane: II. Structural Investigation."* **Macromolecules 34, 1411-1421** (2004)

Publications 2003

3-1 Amara M., Luca S. E., Galéra R.M., Aviani I., Bérar J.F. : *"Orbital degrees of freedom and ordering phenomena in a 4f system"* **J. Solid State Chem. 171** 1-2 (2003) pp.69-75

3-2 Antion C., Donnadieu P., Tassin C., Perrard F., Deschamps A., Pisch A. : *"Hardening precipitation in a Mg-4Y-3Re alloy"* **Acta Materialia 51** 18 (2003) pp.5335-5348 (2003)

3-3 Biego B. David L., Girard-Reydet E., Lucas J.M., Denizard O. : *"Multiscale Morphology and thermomechanical history of PVC. "* **Polymer International** (2003) in press

3-4 Blanquet E., Donnadieu P., Schouler M.C., Simon J.P., Maret M., Pons M., Cocheteau V., Caussat B., Scheid E., Mur P., Semeria M.N. : *"Macroscopic and microscopic investigations on the LPCVD fabrication of silicon nanodots on oxidized silicon wafers"* **Conference EURO-CVD 14** to be published

3-5 Boudet N., Bérar J.F., Blanquart L., Breugnon P., Caillot B., Clemens J.C., Koudobine I., Delpierre P., Mouget C., Potheau R., Valin I. : *"XPAD: a hybrid pixel detector for x-ray diffraction and diffusion "* **NIM A 510** 1-2 (2003) pp.41-44

3-6 Boulle A., Masson O., Guinebretiere R., Dauger A. : *"A new method for the determination of strain profiles in epitaxic thin films using X-ray diffraction."* **J. Appl. Cryst. 36** (2003) pp.1424-1431

3-7 Coulet M.V., Simonet V., Calzavara Y., Testemale D., Hazemann J.L., Raoux D., Bley F., Simon J.P. : *"Correlation between density variation and electrical conductivity in supercritical selenium probed by small angle x-ray scattering"* **J. Chem. Phys. 118** 24 (2003) 707324

3-8 Deschamps A., Bley F., Livet F., Fabrègue D., David L. : *"In-situ small-angle X-ray scattering study of dynamic precipitationin an Al-Zn-Mg-Cu alloy"* **Phil. Mag. 83** 6 (2003) pp.677-692

3-9 Deschamps A., Militzer M., Poole W.J. : *"Comparison of precipitation kinetics and strengthening in an Fe-0.8% Cu alloy and a 0.8% Cu-containing low-carbon steel"* **ISIJ International 43** 11 (2003) pp.1826-1832

3-10 Dumont D., Deschamps A., Bréchet Y. : *"On the relationship between microstructure and toughness in AA7050 aluminum alloy"* **Materials Science and Engineering A356** (2003) pp.326-336

3-11 Ehrburger-Dolle F., Bley F., Geissler E., Livet F., Morfin I., Rochas C. : *"Filler networks in elastomers"* **Macromolecular Symposia 200** (2003) pp.157-167

3-12 Ehrburger-Dolle F., Morfin I., Geissler E., Bley F., Livet F., Vix-Guterl C., Saadallah S., Parmentier J., Reda M., Patarin J., Iliescu M., Werckmann J. : *"Small-angle X-ray scattering and electron microscopy investigation of silica and carbon replicas with ordered porosity"* **Langmuir 19** (2003) pp.4303-4308

3-13 Gastildi J., Agliozzo S., Letoublon A., Wang J., Mancini L., Klein H., Haertwig J., Baruchel J., Fisher I.R., Sato T., Tsai A.P., De Boissieu M. : *"Degree of structural perfection of icosahedral quasicrystalline grains investigated by synchrotron X-ray diffractometry and imaging techniques"* **Phil. Mag. 83** (2003) pp.1-29

3-14 Goerigk G., Haubold H.G., Lyon O., Simon J.P. : *"Anomalous small-angle X-ray scattering in materials science"* **J. Appl. Cryst. 36** (2003) pp.425-429

3-15 Grenier S., Letoublon A., Proietti M.G., Renevier H., Gonzalez L., Garcia J.M., Priester C., Garcia J. : *"Grazing incidence diffraction anomalous fine structure of self-assembled semiconductor nanostructures"* **NIM B 200** (2003) pp.24-33

3-16 Hennet L., Thiaudiere D., Landron C., J, Berar F., Saboungi M.L., Matzen G., Price D.L. : *"Anomalous X-ray scattering on molten levitated samples"* **NIM B 207** (2003) pp.447-452

3-17 Hennet L., Thiaudiere D., Landron C., Melin P., Price D.L., Coutures J.P., Bérar Saboungi M.L. : *"Melting Behavior of levitated Y2O3."* **Appl. Phys Lett. 83** (2003) pp.3305-3307

3-18 Herrera Negrette N., Letoffe J.M., Puteaux J.L., David L., Bourgeat-Lami E. : *"Aqueous Dispersions of Silane-Functionalized Laponite Clay Platelets. A first step towards the elaboration of water-based polymer/clay nanocomposites."* **Langmuir, In** press.

3-19 Hosokawa S., Wang Y., Bérar J.F., Sakurai M., Pilgrim W.C. : *"Anomaloux X-ray scattering studies on glassy GexSe(1-x) over a wide concentration range including the stiffness transition composition."* **J. Non-Cryst. Solids 326-327** (2003) pp.394-398

3-20 Hosokawa S., Wang Y., Sakurai M., Bérar J.F., Pilgrim W.C., Murase K. : *"Rigidity transitions and intermediate structures of Ge-Se glasses - An anomaloux X-ray scattering study."* **NIM B 199** (2003) pp.165-168

3-21 Livet F., Bley F., Ehrburger-Dolle F., Geissler E., Lebolloc'h D., Schulli T. : *"Ultra small-angle X-ray scattering: conditions, limits and results in speckle experiments"* **J. Appl. Cryst. 36** (2003) pp.774-777

3-22 Lorimier J., Guigue-Millot N., Bernard F., Niepce J.C., Bérar J.F. : *"Mixed valences in nanometric ferrites investigated by resonnant powder diffraction "* **J. Appl. Cryst. 36** (2003) pp.301-307

3-23 Létoublon A., Renevier H., Proietti M.G., Priester C., Garcia J.M., Gonzalez L. : *"Grazing incidence diffraction anomalous fine structure: a tool for investigating strain distribution and interdiffusion in InAs/InP quantum wires."* **Physica E 17** (2003) pp.541-542

3-24 Millot N., Aymes D., Bernard F., Niepce J.C., Traverse A., Bouree F., Cheng B.L., Perriat P. : *"Particle size dependency of ternary diagrams at the nanometer scale: evidence of TiO2 clusters in Fe-Based spinels"* **J. Phys. Chem. B 107** (2003) pp.5740-5750

3-25 Moinard D., Taton D., Gnanou Y., Rochas C., Borsali R. : *"SAXS from four-arm polyelectrolyte stars in semi-dilute solutions"* **Macromolecular Chemistry and Physics 204** (2003) pp.89-97

3-26 Morfin I., Horkay F., Basser P.J., Bley F., Ehrburger-Dolle F., Hecht A.-M., Rochas C., Geissler E. : *"Ion condensation in a polyelectrolyte gel"* **Macromolecular Symposia 200** (2003) pp.227-233

3-27 Nicolas M., Deschamps A. : *"Characterisation and modelling of precipitate evolution in an AlZnMg alloy during non-isothermal heat treatments"* **Acta Materialia 51** 20 (2003) pp.6077-6094

3-28 Renevier H., Grenier S., Arnaud S., Bérar J.F., Caillot B., Hodeau J.L., Létoublon A., Proietti M.G., Ravel B., Gonzalez L. : *"Diffraction anomalous fine-structure spectroscopy at beamline BM2 at the European Synchrotron Radiation Facility."* **J. Synchrotron Rad. 10** (2003) pp.435-444

3-29 Spalla O., Lyonnard S., Testard F. : *"Analysis of the small-angle intensity scattered by a porous and granular medium"* **J. Appl. Cryst 36** (2003) pp.338-347

3-30 Teixeira A.V., Morfin I., Ehrburger-Dolle F., Rochas C., Geissler E., Licinio P., Panine P. : *"Scattering from dilute ferrofluid suspensions in soft polymer gels"* **Phys. Rev. E 67** (2003) 021504 1-7

3-31 Teixeira A.V., Morfin I., Ehrburger-Dolle F., Rochas C., Panine P., Licinio P., Geissler E. : *"Structure and magnetic properties of dilute ferrofluids suspended in gels"* **Comp. Sci. and Techn. 63** (2003) pp.1105-1111

Publications 2002

2-1 Bertoncini P., Wetzel P., Berling D., Mehdaoui A., Loegel B., Peruchetti J.C., Gewinner G., Pierron-Bohnes V., Bérar J.F., Renevier H. : *"Strain determination in ultrathin bcc Fe layers on Si(001) by X-ray diffraction "* **Phys. Rev. B 65** (2002) 155425

2-2 Bigault T., Bocquet F., Labat S., Thomas O., Renevier H. : *"Chemically diffuse interface in (111)Au-Ni multilayers : an anomalous x-ray diffraction analysis"* **Appl. Surf. Sci. 188** (2002) pp.110-114

2-3 Buron M., Collet E., Lemee-Cailleau M. H., Cailleau H., Luty T., Ravy S., Bérar J.F. : *"One-dimensionality and neutral-to-ionic transition of some mixed-stack charge-transfer complexes "* **J. Phys. IV 12** (2002) pp.357, ECRYS-2002, 2-7Sept, Saint-Flour, France

2-4 Bérar J.F., Blanquart L., Boudet N., Breugnon P., Caillot B., Clemens J.C., Koudobine I., Delpierre P., Mouget C., Potheau R., Valin I. : *"Pixel detectors : new detectors for X-ray scattering "* **J. Phys. IV 12** (2002) pp.385, RX 2001 4-7 Dec. 2001, Strasbourg

2-5 Bérar J.F., Blanquart L., Boudet N., Breugnon P., Caillot B., Clemens J.C., Koudobine I., Delpierre P., Mouget C., Potheau R., Valin I. : *"A pixel detector with large dynamic range for high photon counting rates "* **J. Appl. Cryst. 35** (2002) pp.471-476 (2002)

2-6 Collet E., Lemee-Cailleau M. H., Buron-Le Cointe M., Cailleau H., Ravy S., Luty T., Bérar J.F., Czarnecki P., Karl N. : *"Direct evidence of lattice-relaxed charge transfer exciton strings "* **Europhysics Letters 57** 12 (2002) pp.67-73 (2002)

2-7 De Boissieu M., Takakura H., Bletry J., Guo J.Q., Tsai A.P. : *"Phason fluctuations in i-AlPdRe and i-CdYb phases"* **J. Alloys and Compounds 342** (2002) pp.265-270

2-8 Delpierre P., Berar J.F., Blanquart L., Boudet N., Breugon P., Caillot B., J.C.Clemens., Mouget C., Potheau R., Valin I. : *"Large Surface X-Ray Pixel Detector"* **IEEE Trans. Nucl. Science 49** (2002) 4 pp.1709, NSS-MIC/IEEE San-Diego (USA), Nov.4-10, 2001

2-9 Dubourdieu C., Pantou R., Weiss F., Senateur J.-P., Dooryhee E., Hodeau J.-L., Kobernik G., Haessler W. : *"Structural and dielectric properties of (BaTiO3//SrTiO3)15 superlattices grown by MOCVD "* **Ferroelectrics 268** (2002) pp.137-142

2-10 Etienne S., David L. : *"Introduction à la physique des polymères"* **Edited by Dunod, Paris, (2002) Chapter** 8

2-11 Frey F., Weidner E., Hradil K., Boissieu M. De, Letoublon A., Mcintyre G., Currat R., Tsai A.P. : *"Temperature dependence of the 8-A superstructure in decagonal Al-Co-Ni"* **J. Alloys and Compounds 342** (2002) pp.57-64

2-12 Geissler E., Hecht A.-M., Rochas C., Horkay F., F.Bley., Livet F. : *"Structure and dynamics of silica-filled polymers by SANS and SAXS"* **Macromolecular Symposia 190** (2002) pp.23-32

2-13 Grenier S., Proietti M.G., Renevier H., Gonzalez L., Garcia J.M., J.Garcia. : *"Grazing Incidence diffraction anomalous fine structure of InAs/InP(001) self-assembled quantum wires"* **Europhysics Letters 57** (2002) 4 pp.499-505

2-14 Guigue-Millot N., Bernard F., Niepce J.C., Traverse A., Perriat P. : *"Phenomenes de segregation dans les ferrites de titane nanometriques : apports complementaires de differentes techniques experimentales (DRX resonnante, Diffraction de neutrons, EXAFS...) "* **J. Phys. IV 12** (2002) pp.473, RX 2001, 4-7 Dec. 2001, Strasbourg

2-15 Holderer O., David L., Delichere P., Epicier T., Esnouf C., Fuchs G. : *"Convergent analytical approach for the caracterisation of solutions and deposits of nano-colloids "* **J. Phys. IV 12** (2002) pp.473, RX 2001, 4-7 Dec. 2001, Strasbourg

2-16 Hosokawa S., Pilgrim W.-C., Kawakita Y., Wang Y., Bérar J.F., Murase K. : *"Anomalous X-ray scattering studies on intermediate structures in chalcogenide glasses- glassy GexSe1-x across the stiffness threshold composition"* **Phys. Chem. Glasses 43C** (2002) pp.175-180

2-17 Hosokawa S., Wang Y., Bérar J.-F., Pilgrim W.-C., Murase K. : *"Anomalous X-ray scattering studies on glassy GexSe1-x across the stiffness threshold composition x=0.20"* **Z. Phys. Chem. 216** (2002) pp.1219-1238

2-18 Hubert L., David L., Séguéla R., Vigier G., Corfias-Zuccali C., Germain Y. : *" Physical and Mechanical Properties of Polyethylene for Pipes in relation to Molecular Architecture. Part II. Short-Term*

Creep of Isotropic and Drawn Materials," **J. Appl. Polymer Science 84** (2002) pp.2308-2317

2-19 Ibanes C., David L., Seguela R., Vigier G., Epicier T., De Boissieu M., Rochas C., Robert G. : *" Morphology and mechanical properties of Nylon 6 nanocomposite fibers"* **Polymer films and Fibers, Montreal, Canada septembre** 2002

2-20 Le Parc R., Champagnon B., David L., Faivre A., Levelut C., Guenot P., Hazemann J.L., Rochas C., Simon J.P. : *"Temperature dependence of the density fluctuations of silica by small-angle X-ray scattering "* **Philosophical Magazine B 82** (2002) pp.431-438

2-21 Lemee N., Dubourdieu C., Delabouglise G., Senateur J.-P., Laroudie F. : *"Semiconductive Nb-doped BaTiO3 films grown by pulsed injection metalorganic chemical vapor deposition "* **J. Crystal Growth 235** (2002)1-4 pp.347-51

2-22 Levelut C., Faivre A., Le Parc R., Champagnon B., Hazemann J.L., David L., Rochas C., Simon J.P. : *"Influence of thermal aging on density fluctuations in oxide glasses measured by small-angle X-ray scattering"* **J. Non-Cryst Solids, 307-310 (2002) 426-435**

2-23 Livet F., Bley F., Simon J.-P., Caudron R., Mainville J., Sutton M., Lebolloc'h D. : *"Statics and kinetics of the ordering transition in the AuAgZn2 alloy "* **Phys. Rev. B 66 (2002) 134108**

2-24 Luca S.E., Amara M., Galéra R.M., Bérar J.F. : *"Multipolar X-ray diffraction study of the canted magnetic structure of TbMg"* **J. Phys. Condens Matter 14** (2002) 377-387

2-25 Maier A., Riedlinger B., Treubel F., Maret M., Albrecht M., Beaurepaire E., Tonnerre J.M., Schatz G. : *"Nanostructured CoPt3(111) films grown on WSe2(0001)"* **J. Magnetism and Magnetic Materials 240** (2002) pp.377-379

2-26 Nassif V.M., Carbonio R.E., Hodeau J.L., Dooryhee. E. : *"X-ray structural determination of a multilayered magnetic dielectric ceramic Ba42Ti51Fe200174 in the BaO-TiO2-Fe2O3 system. "* **J. Solid State Chemistry 166 (2002) pp.400-414**

2-27 Nicolas M., Deschamps A. : *"Precipitate microstructure in the heat-affected zone of Al-Zn-Mg MIG-welds and evolution during post-welding heat treatments"* **Materials Science Forum 396-402** (2002) pp.1561-1566 (Proceedings of the 8th Int. Conf. on Aluminium Alloys, Cambridge, UK, 2002

2-28 Phé B-H., Bounor-Legare V., David L., Michel A : *" Optimization of the nanoscaled morphology of organic hybrid materials elaborated by reactive extrusion"* **Polymer modification, degradation, and stabilization, (Budapest, Hongrie, 30 juin-4** juillet 2002)

2-29 Phé B-H., Bounor-Legare V., David L., Michel A. : *" Control of the morphology of organic-inorganic hybridmaterials elaborated by reactive extrusion."* **Polymer Processing Symposium, PPS-18 (Guimaraes, Portugal, 16-20** juin 2002)

2-30 Rannou P., Dufour B., Travers J.P., Pron A., Djurado D., Janeczek H., Sek D. : *"Temperature-induced transitions in doped polyaniline: Correlation between glass transition, thermochromism and electrical transport"* **J. Phys. Chem. B 106 (2002) pp.10553-10559**

2-31 Ravy S. : *"Diffusion diffuse des rayons X : des zones de Guinier-Preston aux oscillation de Friedel "* **J. Phys. IV 12 (2002) p7, RX 2001 4-7 Dec. 2001** Strasbourg

2-32 Schappacher M. De Souza Lima R. Borsali S. Leccommandoux A. M., Deffieux P., Lindner C. Rochas F. Checot, C., Moinard : *"Small Angle Neutrons and x-rays scattering from linear and star Brush-like polymer"* **Polymers preprint (2001) 42(2). Orlando (USA). avril** 2002

2-33 Vendier L., Sciau Ph., Dooryhee E. : *"Apport de la diffraction des rayons X a l'etude d'engobes de poteries gallo-romaines "* **J. Phys. IV 12 (2002) p587, RX 2001 4-7 Dec. 2001** Strasbourg

Publications 2001

1-1 Berthon S., Barbieri O., Ehrburger-Dolle F., Geissler E., Achard P., Bley F., Hecht A-M., Livet F., Pajonk G.M., Pinto N., Rigacci A., Rochas C. : *"DLS and SAXS investigations of organic gels and aerogels "* **J. Non-Cryst. Solids 285** (2001) pp.154-161

1-2 T. Bigault, Bocquet F., Labat S., Thomas O., Renevier H. : *"Interfacial structure in (111) Au:Ni multilayers investigated by anomalous x-ray diffraction "* **Phys. Rev. B 64** (2001) 125414

1-3 Chacon C., Isnard O., Berar J.F. : *"X-Ray anomalous diffraction study of the crystal structure of Y(Co,Ni)4B Compounds"* **Materials Science forum 378-381** (2001) pp.434-439

1-4 Deschamps A., Militzer M., Poole W.J. : *"Precipitation kinetics and strengthening of a Fe-O.8wt % Cu alloy"* **ISIJ International 41** (2001) pp.196-205

1-5 Dooryhee E., Hodeau J.L., Nemoz M., Rodriguez J. A., Dubourdieu C., Pantou R., Rosina M., Weiss F., Senateur J.P., Audier M., Roussel H., Lindner J. : *" Modeling the diffraction profiles of CVD-grown perovskite oxide superlattices "* **J. Phys. IV 11** (2001), pp.267-272

1-6 Dubourdieu C., Rosina M., Audier M., Weiss F., Senateur J.P., Dooryhee E., Hodeau J.L. : *"Application of pulsed liquid-injection MOCVD to the growth of ultrathin epitaxial oxides for magnetic heterostructures"* **Thin Solid Films 400** (2001) pp.81-84

1-7 Dubourdieu C., Rosina M., Roussel H., Weiss F., Senateur J.P., Hodeau J.L. : *"Pulsed liquid-injection metalorganic chemical vapor deposition of (La0.7Sr0.3MnO3/SrTiO3)15 superlattices"* **Appl. Phys. Lett. 79 (2001) pp.1246-1248**

1-8 Dufour B., Rannou P., Fedorko P., Djurado D., Travers J.P., Pron A. : *"Effect of plasticizing dopants on spectroscopic properties, supramolecular structure, and electrical transport in metallic polyaniline"*

Chemistry of Materials 13 (2001) pp.4032-4040 (2001)

1-9 Ehrburger-Dolle F., Al. : *"Role of fractal features in the structure-property relationships of carbon black filled polymers"* **Mater. Res. Soc. Symp. Series, 661** KK7.4.1-10(2001)

1-10 Ehrburger-Dolle F., Hindermann-Bischoff M., Livet F., Bley F., Rochas C., Geissler E : *"Anisotropic ultra-small-angle X-ray scattering in carbon black filled polymers"* **Langmuir 17(2)329-334** (2001)

1-11 Einarsrud M.A., Nilsen E., Rigacci A., Pajonk G.M., Buathier S., Valette D., Durant M., Chevalier B., Nitz P., Ehrburger-Dolle F. : *"Strengthening of silica gels and aerogels by washing and aging processes "* **J. of Non-Cryst. Solids 285** 1-7(2001)

1-12 Favre-Nicolin V., Bos S., E. Lorenzo J., Hodeau J-L., Berar J-F., Monceau P., Currat R., Levy F., , Berger H. : *"Structural Evidence for Ta-Tetramerization Displacements in the Charge-Density-Wave Compound (TaSe4)2I from X-Ray Anomalous Diffraction "* **Phys. Rev. Letters 87** (2001) 015502

1-13 Garcia J., Subias G. : *"Valence state and local structure in magnetite and Ca-doped manganites"* **OYANAGI H., BIANCONI A. - Physics in Local Lattice Distortions, (2001) 357-3651-56396-984-X, American Institute of** Physics

1-14 Garcia J., Subias G., Proietti M.G., Blasco J., Renevier H., Hodeau J.L., Joly Y. : *"Absence of charge ordering below the Verwey transition temperature in magnetite."* **Phys. Rev. B 63** (2001) 054110

1-15 Geissler E., Hecht A.-M., Rochas C., Horkay F., Bley F., Livet F., Sutton M. : *"Small angle scattering and the structure and dynamics of filled and unfilled rubbers"* **Mater. Res. Soc. Symp. Series, 661** (2001) KK7.4.1-10

1-16 Grenier S., Proietti M.G., Renevier H., Gonzalez L., Garcia J.M., Gerard J.M., , Garcia J. : *"Glancing-angle diffraction anomalous fine structure of InAs quantum dots and quantum wires"* **J. Synchrotron Rad. 8** (2001) pp.536-538

1-17 Grenier S., Renevier H., Tonnerre J.M., Fisher H. : *" A FexMn1-x/Ir(001) multilayer probed by EXAFS and DAFS"* **J. Synchrotron Rad. 8** (2001) pp.886-888

1-18 Hecht A.M., Horkay F., Geissler E. : *"Structure of polymer solutions containing fumed silica "* **Physical Review E 64** (2001) 041402

1-19 Heinrich M., Rawiso M., Zilliox J.G., Lesieur P., Simon J.P. : *"Small angle X-ray scattering from salt-free solutions of star-branched polyelectrolytes "* **Eur. Phys. J. E 4** (2001) pp.131-142

1-20 Hodeau J.L., Favre-Nicolin V., Bos S., Renevier H., Lorenzo E., Bérar J.F. : *"Resonant diffraction "* **Chem. Rev. 101** (2001) pp.1843-67

1-21 Hosokawa S. : *" Atomic and electronic structures of glassy GexSe1-x around the stiffness threshold composition"* **J. Optoelectronics and Advanced Materials 3** (2001) pp.199-214

1-22 Lorimier J., Bernard F., Isnard O., Niepce J.-C., Bérar J.F. : *"Anomalous valence contrast of metal transition in nanocrystalline ferrite"* **Materials Science forum 378-381** (2001) pp.594-599

1-23 Létoublon A., De Boissieu M., Boudard M., Mancini L., Castaldi J., Hennion B., Caudron R., Bellissent R. : *" Phason elastic constants of the icosahedral Al-Pd-Mn phase derived from diffuse scattering measurements"* **Phil. Mag. Letters 81** (2001) pp.273-283

1-24 Nicolas M., Werenskiold J.C., Deschamps A., Bley F., Livet F., Simon J.P. : *"Study of precipitate microstructures in the heat-affected zones of a welded Al-Zn-Mg alloy"* **Conf: Euromat 2001** to appear in Scripta Metallurgica

1-25 Pachot S., Darie C., Berar J.F., Bordet P., Bougerol-Chaillout C. : *"Refinement of imcommensurate misfit compounds : Sr14-xCaxCu24O41"* **Materials Science forum Vols. 378-381** (2001) pp.638-643

1-26 Pantou R., Dubourdieu C., Weiss F., Senateur J.-P., Kobernik G., Haessler W. : *"Electrical properties of (BaTiO3//SrTiO3)15 superlattices grown by MOCVD"* **J. Phys. IV 11** (2001) pp.313-17

1-27 Ravel B., Grenier S., Renevier H., Eom C-B. : *"Valence selective DAFS measurements of Mn in La1/3Ca2/3MnO3 "* **J. Synchrotron Rad. 8** (2001) pp.384-386

1-28 Ravy S., Rouziere S., Pouget J.P., Brazovskii S. : *" Friedel oscillations and charge-density waves pinning in quasi-one-dimensional conductors"* **Synthetic Metals 120** (2001) pp.1075-1076

1-29 Renevier H., Joly Y., Garcia J., Subias G., Proietti M.G., Hodeau J.L., Blasco J. : *" DAFS of forbidden Bragg reflections : charge localization and structure of the octahedral site in magnetite"* **J. Synchrotron Rad. 8** (2001) pp.390-392

1-30 Rigacci A., Ehrburger-Dolle F., Geissler E., Chevalier B., Sallee H., Achard P., Barbieri O., Berthon S., Bley F., Livet F., Pajonk G.M., Pinto N., Rochas C. : *"Investigation of the multiscale structure of silica aerogels by SAXS "* **J. Non-Cryst. Solids 285** (2001) 187

1-31 Rosina M., Dubourdieu C., Audier M., Doorhee E., Hodeau J.L., Weiss F., Fröhlich F. : *"Structural characterisation of manganite superlattices. "* **J. Phys. IV 11 (2001) pp.122, TFDOM'2** Int Conf , Autrans-F, Oct. 2001

1-32 Rosina M., Dubourdieu C., Weiss F., Senateur J.-P., Frohlich K. : *"Structural properties of (La0,7Sr0,3MnO3//SrTiO3)15 superlattices prepared by pulsed injection-MOCVD"* **J. Phys. IV 11** (2001) pp.341-7